

UNCLASSIFIED

AD 4 6 4 3 3 4

DEFENSE DOCUMENTATION CENTER

FOR

SCIENTIFIC AND TECHNICAL INFORMATION

CAMERON STATION ALEXANDRIA, VIRGINIA



UNCLASSIFIED

NOTICE: When government or other drawings, specifications or other data are used for any purpose other than in connection with a definitely related government procurement operation, the U. S. Government thereby incurs no responsibility, nor any obligation whatsoever; and the fact that the Government may have formulated, furnished, or in any way supplied the said drawings, specifications, or other data is not to be regarded by implication or otherwise as in any manner licensing the holder or any other person or corporation, or conveying any rights or permission to manufacture, use or sell any patented invention that may in any way be related thereto.

4 6 4 3 3 4

April 1965

ERRATA - May 1965

The following corrections are applicable to AFFDL-TR-65-32, Experimental Oxygen Concentrating System, UNCLASSIFIED Report, April 1965:

Page iii

The third from the last sentence should read: "This unit has a capacity for humidifying 1 SCFM of room air to a dew point of 95°F."

Page 24

The last sentence of the fourth paragraph should refer to the APPENDIX instead of Section VIII.

Page 35

The last two sentences of the last paragraph should read: "After 225 hours of accumulated operating time, a 6.3 hour experimental run was made with an inlet air pressure of 8.0 psia. The results presented in Figure 19 (b) show that the performance curve taken at 8.0 psia (after 3 hours operation at this pressure) is very similar to the generator performance observed after the air inlet pressure was returned to 14.7 psia."

Page 37

The last sentence of the third paragraph should be changed to read: "Also, each cell has a slightly different environment, resulting from its position in the series stack, and they may see slightly different air flows due to small variations that occur during fabrication of the ducts, etc."

Page 39

The last sentence of the fourth paragraph should read: "This would indicate that their lower voltage levels resulted from an effect associated with operation at less than atmospheric pressure."

Air Force Flight Dynamics Laboratory
Research and Technology Division
Air Force System Command
Wright-Patterson Air Force Base, Ohio

AFFDL-TR-65-32

EXPERIMENTAL OXYGEN CONCENTRATING SYSTEM

R. A. WYNVEEN
K. M. MONTGOMERY
TRW INC.

**TECHNICAL REPORT AFFDL-TR-65-32
APRIL 1965**

AIR FORCE FLIGHT DYNAMICS LABORATORY
RESEARCH AND TECHNOLOGY DIVISION
AIR FORCE SYSTEMS COMMAND
WRIGHT-PATTERSON AIR FORCE BASE, OHIO

NOTICES

When Government drawings, specifications, or other data are used for any purpose other than in connection with a definitely related Government procurement operation, the United States Government thereby incurs no responsibility nor any obligation whatsoever; and the fact that the Government may have formulated, furnished, or in any way supplied the said drawings, specifications, or other data, is not to be regarded by implication or otherwise as in any manner licensing the holder or any other person or corporation, or conveying any rights or permission to manufacture, use, or sell any patented invention that may in any way be related thereto.

Qualified requesters may obtain copies of this report from the Defense Documentation Center (DDC), (formerly ASTIA), Arlington Hall Station, Arlington 12, Virginia.

Foreign announcement and dissemination of this report is not authorized.

DDC release to CFSTI is not authorized.

The distribution of this report is limited because the report contains technology identifiable with items on the strategic embargo lists excluded from export or re-export under U. S. Export Control Act of 1949 (63 STAT. 7) as amended (50 U. S. C. App. 2020.2031) as implemented by AFR 400-10.

Copies of this report should not be returned to the Research and Technology Division unless return is required by security considerations, contractual obligations, or notice on a specific document.

EXPERIMENTAL OXYGEN CONCENTRATING SYSTEM

R. A. Wynveen

K. M. Montgomery

FOREWORD

This report was prepared by the New Product Research Department, Thompson Ramo Wooldridge, Inc. under USAF Contract No. AF 33(615)-1856. This contract was initiated under Project No. 6146, "Atmosphere and Thermal Control", Task No. 614603, "Oxygen and Nitrogen, Concentration and Storage". The program was funded by In-House Laboratory Independent Research Funds and administered under the direction of the Flight Dynamics Laboratory, Research and Technology Division, Mr. David A. Geiger, task engineer.

Dr. Richard A. Wynveen, Senior Engineering Specialist, and Mr. Keith M. Montgomery, Research Engineer, were the principle project engineers for Thompson Ramo Wooldridge Inc.

The authors acknowledge the assistance of the following TRW consultants: Mr. Russ Englehaupt and Mr. Steve Gittinger, Designers, and Mr. Warren Wade, Senior Engineering Specialist, all of TRW's New Product Research Department.

Special acknowledgement is included for Mr. Roger Mason, New Product Research Department Technician, who assisted in conducting the laboratory experimental tests.

The manuscript was released by the authors in March 1965 for publication as an RTD technical report.

This technical report has been reviewed and is approved.


T.J. Baker
Asst. for Research and Technology
Vehicle Equipment Division

ABSTRACT

A program to design, fabricate, and test a laboratory model of an oxygen concentrator, capable of generating 0.20 lb/hr of pure oxygen by electro-chemically concentrating it from air, was successfully conducted. The fabricated model consisted of 26 series-connected cells. Four of the cells, tested before incorporation into the 26-cell unit, demonstrated an oxygen generation rate of 0.10 lb/hr. A 26-cell unit operating at an equivalent unit cell output would produce nearly 0.68 lb/hr, over three times the design level. The 26-cell unit itself was operated at a maximum output of about 0.56 lb/hr for only a short period of time because at this level the heat generated was in excess of the heat removal systems' capacity. At the completion of the contractual test program, over 700 hours had been accumulated on the original four cells, about 345 hours of which were logged while functioning as part of the 26-cell unit. During its 345 hours of operation, the 26-cell unit had an over-all average output of 0.22 lb/hr. The concentrator was shown to function properly at 6.5 - 15.5 psia pressures, with little variation in the power required for a given oxygen output. For optimum performance, the generator required an air flowrate of at least 2.5 times the theoretical minimum. Oxygen purity was over 99.5%, except when the air compartment pressure exceeded the oxygen compartment pressure by more than 1 - 6 psi, the limiting pressure differential being somewhat dependent upon the moisture level and compression of the electrolyte matrix. Compared to the laboratory model which weighs about 28 pounds and consumes 240 - 300 watts of power, an optimized concentrator with the same 0.2 lb/hr oxygen output would weigh about 13 pounds and consume 150 watts of power. Also included in this program was the design, fabrication, and testing of a humidifier that would operate under airborne conditions. This unit had a capacity for humidifying 1 SCFM of room air to a dew point of 95%. A control system for the generator consisted of an air supply a power supply, and heat removal facilities. Instrumentation was provided for measuring and controlling gas flows, pressures, temperatures, and dew points and for monitoring cell voltages.

TABLE OF CONTENTS

	<u>Page</u>
I. INTRODUCTION	
Background	1
Objective	1
Approach	1
II. ELECTROCHEMICAL OXYGEN CONCENTRATING	
Cell Operation	3
Electrochemical Principles	5
Summary of Prior Technology	7
III. DESIGN AND FABRICATION	
General Design Considerations	10
Generator Design Parameters	10
Generator Fabrication	12
Auxiliaries and Instrumentation	19
Test Rig Instrumentation	27
IV. EXPERIMENTAL RESULTS	
Two -Cell and Four-Cell Units	35
Twenty-Six Cell Generator	37
Demonstrated Operating Life	39
Effect of Flowrate	39
Effect of Inlet Pressures	39
Effect of Operating Temperature	41
Oxygen Output	41
Oxygen Purity	41
Stability to Pressure Differentials	42
V. DESIGN ANALYSIS AND RECOMMENDATIONS	
Design Criteria Evaluation	44
Design Improvements	45
Problems and Solutions	46
Design Recommendation	46
VI. SUMMARY	50
VII. REFERENCES	51
APPENDIX - DESIGN CALCULATIONS	52

ILLUSTRATIONS

<u>FIGURE NO.</u>		<u>Page</u>
1	Basic Cell Operation	4
2	Variation of Voltage with Current Oxygen (Output)	6
3	Reproducibility of Single Cell Test Results	8
4	Temperature Versus Vapor Pressure of KOH Solutions	13
5	Generator Components	15
6	Air Compartment of Bi-Polar Plate	17
7	Oxygen Compartment of Bi-Polar Plate	18
8	Twenty-Six-Cell Assembly	20
9	Twenty-Six-Cell Oxygen Generator	21
10	Generator and Control System	22
11	Test Rig Schematic	23
12	Humidifier Assembly	25
13	Water Feed System	26
14	Flow and Pressure Control Panel	28
15	Electrical Instrumentation Panel	30
16	Heat and Humidification Control Panel	31
17	Humidity and Temperature Control	32
18	Air Supply Trap	34
19	Four-Cell Generator Performance	36
20	Laboratory Model in Operation	38
21	Effect of Flowrate	40
22	Effect of Flowrate at Reduced Pressure	40
23	Generator Extended Performance	43
B-1	Bi-Polar Plate Temperature Profile	63
C-1	Theoretical Air Flow Rates	65
D-1	Illustration of Gas Ducts and Ports	66
D-2	Port Passage	66
E-1	Frame Diagram	71
F-1	Dimensional Diagram of Cooling Air Passage	75
F-2	Cooling Air Passage	76

LIST OF TABLES

<u>TABLE NO.</u>		<u>Page</u>
1	0.2 lb/hr Oxygen Generator Design Parameters	14
2	Component and Total Weights	47
3	Comparison of Generator to be Delivered With and Optimized Generator of Same Design	49
C-1	Theoretical Air Flow Rates	65

SECTION I. INTRODUCTION

Background

As a result of TRW's research efforts, a versatile new approach for electro-chemically generating pure oxygen has been conceived and demonstrated. The unique feature of the TRW device is that air is the source of oxygen. Applying a small amount of electrical power while air is being fed into the device results in the separation of oxygen from the inert gases and impurities found in the air. The approach is simple in that only a source of air and electrical power are required to concentrate the oxygen. The device itself is based upon an electrochemical cell design that is inherently lightweight and compact and includes the features necessary for operation independent of orientation relative to gravitational forces. Of the many applications envisioned for the concept, its application as a method for providing oxygen to meet the breathing needs of aviators seems particularly attractive.

Traditionally the reliable source of breathing oxygen for aviators has been provided by supplying a sufficient amount of oxygen for each flight prior to takeoff. Storage and maintenance of quantities of high pressure or cryogenic oxygen onboard aircraft pose significant logistics and safety problems. The maintaining of equipment for production and storage of this oxygen on combat bases poses additional safety hazards and levies a significant cost in training and surveillance.

Objective

A program was initiated to design, fabricate, test and deliver a 0.2 lb/hr laboratory model of the electrochemical oxygen generator. Such an oxygen generator would be capable of meeting the breathing needs of an aviator when combined with a rebreather system and would provide enough excess to replace leakage losses. Included as part of the program was the development of a design recommendation based upon the test results conducted on the program.

Approach

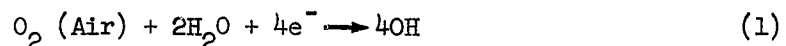
The generator and control system were designed according to technology possessed by TRW prior to initiation of the program. The development of the final 26 cell model of the 0.2 lb/hr oxygen generator proceeded in stages. Initially a 2 cell unit was built to verify the design. This was followed by extensive testing of a 4 cell unit. Ultimately these units were incorporated into the final 26 cell device. Optimizing of the generator geometry was given secondary emphasis and standard components were used for the auxiliaries whenever possible. Testing of the device was also completed in stages going from the lesser to the more taxing operating conditions. The tests performed consisted of varying the air pressure, air flowrate, pressure differential across the cell, and operating temperatures and measuring the effects these variations had on the generator's power requirements. Operation was initiated with air at atmospheric pressure and ultimately demonstrated with air pressure as low as 6.5 psia. The flowrate of air fed to the generator was varied from the point where one fifth of the oxygen in the air passing through the device was separated as pure oxygen to the point where more than one third

of the available oxygen was stripped from the air. The pressure differential was varied from 1 to 6 psi while the operating temperature ranged from room temperature to 125°F. These tests were used to evaluate the generator design and to characterize the effects of operating parameters on its performance.

SECTION II. ELECTROCHEMICAL OXYGEN CONCENTRATING

Cell Operation

The method by which pure oxygen is separated from air can be illustrated with the aid of the simplified cell diagram shown in Figure 1. The basic cell consists of two porous metal electrodes separated by an electrolyte solution of aqueous potassium hydroxide. The electrolyte is held in an absorbent porous material which prevents the solution from leaking through the porous electrodes. Air is passed into the gas compartment over one of the porous electrodes called the cathode. When a DC power supply (e.g., battery) is connected to the cell electrodes, electrons are caused to flow through the cathode. The oxygen molecules from the air react with these electrons and with water molecules from the electrolyte to form hydroxyl ions. The half-cell reaction which occurs at the cathode is given by



The hydroxyl ions migrate under the electromotive force provided by the battery to the other porous electrode termed the anode. At this electrode the ions are discharged to again form oxygen, water, and electrons, according to the half-reaction



The oxygen is now separated from the other gases found in the air. These gases, in turn, pass out the exhaust manifold of the cell. The water released at the anode returns to the electrolyte and the electrons travel through the external circuit back to the cathode where they react with more oxygen. The process continues as long as air and power are provided and as long as the cell moisture balance is maintained within certain limits.

According to Faraday's Law's of Electrolysis, the quantity of oxygen that is consumed from the air and released in the anode compartment is directly proportional to the current (electrons) that is allowed to flow through the cell. The output of a unit can be expressed by the equation

$$W = 6.58 \times 10^{-4} (I)(N) \quad (3)$$

where

W = oxygen output, lb/hr

I = current, amps

N = the number of series connected cells in the unit

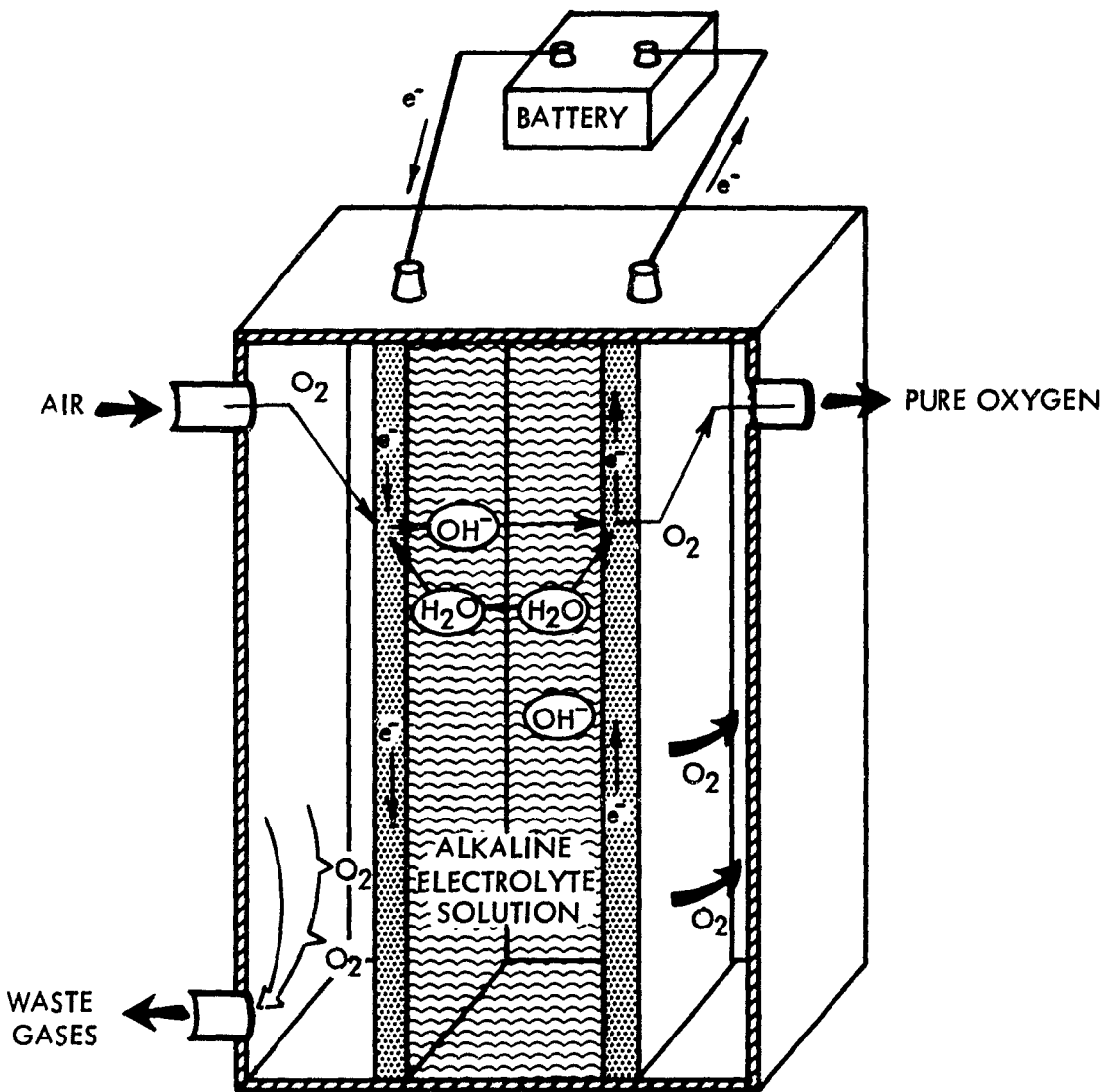


FIGURE 1
BASIC CELL OPERATION

To generate 0.2 lb of oxygen per hour from a single cell required a current flow of 304 amps. If, however, several single cells are electrically connected in series, the current flow required is decreased. In the generator designed under the contract, a total of 26 cells were electrically connected in series. This means that one twenty-sixth of 304 amps of 11.7 amps is required to power the cell assembly. Electrically connecting the 26 cells in series requires that the voltage provided by the power supply be 26 times higher than for a single cell. The oxygen generator was designed to match the particular combination of current and voltage that is available from a conventional 28 volt DC aircraft power supply.

Electrochemical Principles

The actual reaction steps which occur in transforming molecular oxygen into hydroxyl ions are not fully understood. The process is initiated with the chemisorption of the oxygen onto the catalyst surface of the electrode. The overall reaction results in the combination of the chemisorbed oxygen with water and electrons to form hydroxyl ions.

It can be seen that the oxygen evolution reaction given by equation (2) is the reverse of oxygen consumption reaction, shown as equation (1). To accomplish the overall process these two half-cell reactions are combined. From thermodynamic relationships involved with the overall process it can be shown that, if these half-cell reactions were to occur ideally, the application of only a small voltage would be sufficient to separate the oxygen from air. Thus the voltage for pumping oxygen from air at a pressure of 1.0 atmosphere into a compartment filled with pure oxygen at 1.0 atmosphere would ideally be 0.01 volt and the theoretical power input required to separate 0.2 lb of oxygen would be 3.04 watts ($304 \text{ amps} \times 0.01 \text{ volt per cell}$). Unfortunately the actual voltage required is considerably higher than the minimum theoretical voltage. With a practical cell generating 0.2 lb of oxygen per hour, the voltage is about 1.0 volt per cell. This means that the power required is about 304 watts ($304 \text{ amps} \times 1.0 \text{ volt per cell}$).^(a) The additional power requirement is needed to overcome electrode inefficiencies and internal ohmic resistive losses.

Since the current required to produce a given mass of oxygen is fixed (Faraday's Laws of Electrolysis), the only way to reduce power requirements of the oxygen concentrating process is to minimize the voltage drop across the cell. In Figure 2 the relationship between voltage required and current flow (oxygen output) is illustrated. For the purpose of simplification, the voltage loss due to the internal resistance has been omitted. As the cell current increases the voltage difference increases, since each electrode behaves less ideally.

(a)

As will be noted later, various techniques can be used to decrease the required voltage. Both the results under this program and the results of TRW's independent research efforts have shown that the 0.2 lb/hr output could be obtained with a power of 240 watts (0.8 volt per cell) or less.

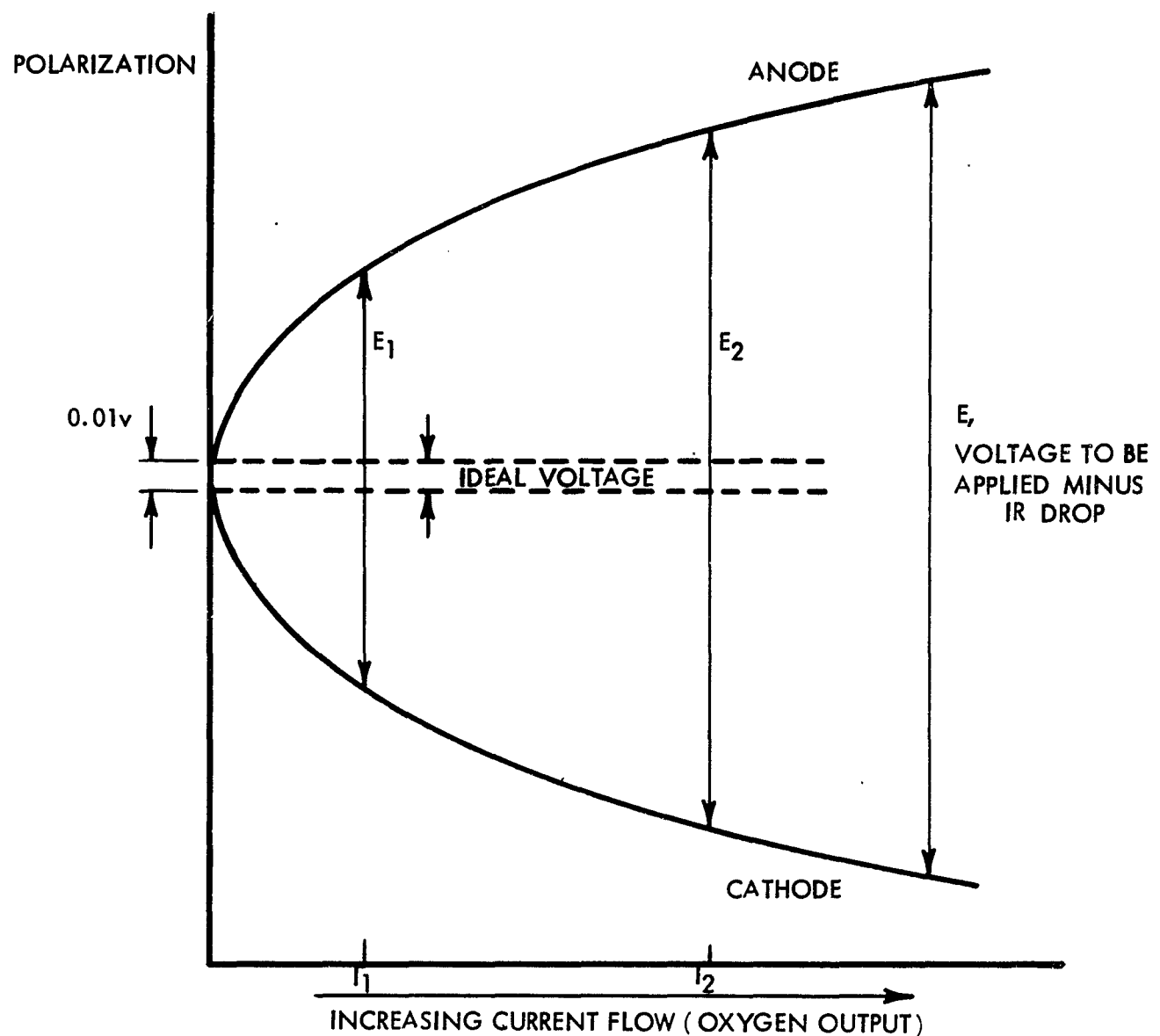


FIGURE 2 VARIATION OF VOLTAGE WITH CURRENT (OXYGEN OUTPUT)

The values of E_1 and E_2 represent the voltage that must be applied to sustain the current (oxygen outputs) denoted by I_1 and I_2 , respectively. The variation of each electrode from its ideal performance is termed polarization. This polarization results from at least two components; (1) polarization due to the slow activation steps of the electrochemical reactions and (2) polarization associated with the slowness of the ionic mass transport processes to and from the electrodes as well as changes in the partial pressure of oxygen in the gas phase.⁽¹⁾

Losses due to internal resistance of the cell result from (1) the resistance of the electrolyte, (2) the contact resistance between the electrodes and the leads, (3) the contact resistance between electrodes and electrolyte if the electrodes are not supported properly, and (4) the resistance of the electrodes themselves. It is important to minimize the internal resistance of the electrochemical cell. Not only does the internal resistance result in the need for increased power required at the cell terminals but it also gives rise to heat which must be dissipated.

Summary of Prior Technology

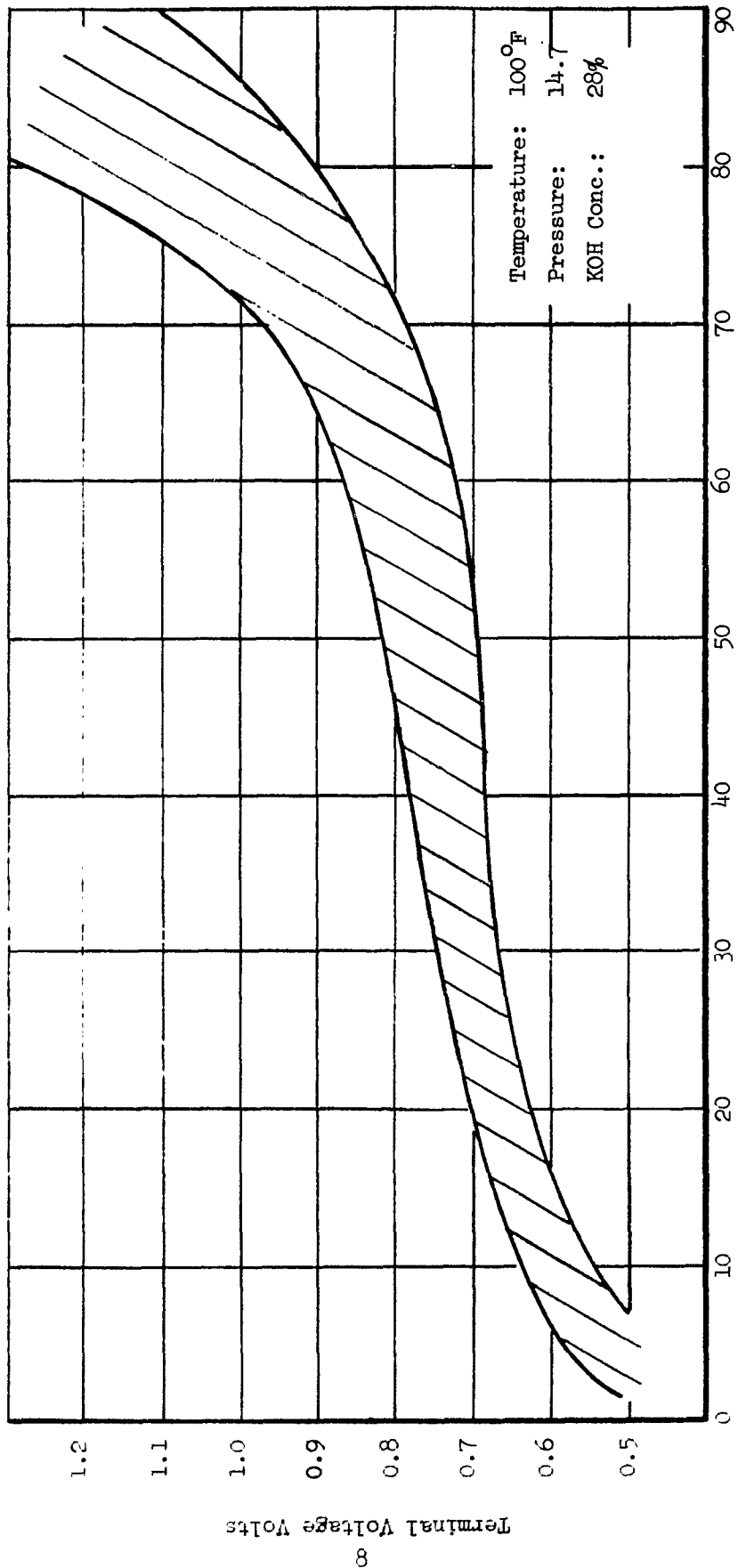
Prior to initiation of the present program TRW had designed and operated many experimental cells. As a result, a basic cell was designed that (1) had a performance considerably above that of the initial cells, (2) could be controlled to deliver oxygen continuously in spite of variations in operating conditions, and (3) could be packaged for operation under the rugged conditions anticipated for field operation. Associated with the last condition was an operational design that was not dependent upon gravity.

A. Single Cell Studies With 2.5 x 2.5 Inch Electrodes

The feasibility of the oxygen concentrating concept was demonstrated by the successful operation of a multitude of small cells. Total operating time of over 1000 hours was logged with most cells operating for 20 to 30 hours. In Figure 3, the range in performance observed with these initial cells is summarized. Cells that had experienced a degradation in performance could be regenerated by either reloading with electrolyte or readjusting the electrolyte concentration to the initial value by passing air with the appropriate water vapor, through the cell. Operating life of single cells was demonstrated to be over 350 hours when the cell electrolyte concentration was held constant. This was accomplished by humidifying the air fed to the cell until the water vapor pressure in the air matched the vapor pressure of the cell electrolyte.

B. Single Cell Studies With 6 x 6 Inch Electrodes

Cells were also constructed with electrodes having larger geometrical areas. Operation of these cells demonstrated that a scale-up in electrode size did not effect the cell performance at low levels of oxygen concentration. However, the performance at higher oxygen outputs per unit of electrode area was only about 2/3 that observed with the smaller cells. Such factors as air distribution, heat removal, and current collection, which directly effect the cell performance, vary in scaling up from smaller to larger cell areas. Thus, a prediction of the performance of larger cells from smaller cell data, cannot, in general, be made from a direct extrapolation. Variations in flow rate were also evaluated on these cells. It was found that air flowrates of 3



to 5 times the theoretical flow had little effect on performance, especially at lower current flows. In these tests, the cell was operated at a given current while variations in the cell voltage were observed as the flowrate was decreased.

C. Multicell Design Studies

An evaluation was made of the factors to be considered in designing larger capacity oxygen generators. Such units result from stacking together multiple single cells. The larger the individual cell electrode areas, the smaller the number of individual cells were required to deliver a given oxygen output. Square, rectangular and circular shaped electrodes had been investigated. Their performances were all comparable. The shape selected for a design, therefore, was determined to be the one which best fit the application environment in which the unit was to operate and which minimized the heat transfer limitations.

At least three basic heat removal designs were considered including (a) circulation of a liquid coolant, (b) evaporative cooling, and (c) conduction to fins cooled with air. The use of cooling fins was considered to be most reliable for a laboratory model that requires a maximum in control over operating variables.

D. Complete Oxygen Generating System Studies

To continually operate the basic electrochemical oxygen generator requires several accessories. The major ones were determined to be a motor-blower to supply the air, a humidifier to add water vapor to the air, a heat removal subsystem to cool the concentrator, and a power supply. Various interrelationships exist between the size and function of the accessories; for example, operation with flowrates more nearly equal to the theoretical flowrate decreases the total mass of air required. This lowers the size of the motor-blower required and decreases the amount of air to be humidified. Flowrates below 3 times the theoretical flowrate, however, increased the generator power requirements and, therefore, the amount of heat to be removed. Final design of a complete generating system was found to depend strongly upon matching the various accessories to best meet the weight, volume, and power conditions established by the oxygen concentrator application.

SECTION III. DESIGN AND FABRICATION

General Design Considerations

Initial design of the multicell generator system was based on prior knowledge possessed by TRW on the oxygen concentrating concept. Primary emphasis was placed on obtaining a reliable and flexible regulating system that would maintain the oxygen production rate at a controllable level. The generator itself received the major emphasis. The auxiliaries were standard off the shelf items wherever possible. This approach permitted a maximum amount of time to be spent in testing of the generator. The optimization of size, weight, and power penalties were given secondary emphasis in this initial design.

Fabrication of the multicell generator was accomplished according to the initial design in steps progressing toward the full size system required for delivery to the Air Force. This involved the building of a few smaller multicell units which were eventually incorporated into the 0.2 lb/hr unit. The deliverable 0.2 lb/hr system was fabricated so that the component cells could be easily disassembled and separated. This facilitated maintenance and made it relatively easy to change the number of cells in the unit.

Generator Design Parameters

A. Electrical Power Requirements

In previous single cell investigations it has been observed that current densities near 50 to 125 amps per sq. ft. (ASF) could be obtained with cell potentials of 0.8 to 1.2 volts. The actual value was dependent upon operating parameters such as temperature, air flowrate, and air pressure. While the lower voltages obtained with selected single cells under optimum conditions represent a goal to be sought, the more rigid operating conditions (e.g., air inlet pressures of 6.5 psia) indicated a more conservative level should be selected for the large capacity generator. A design point of 35 ASF was selected with the assumption that about 1.0 volt would be required per cell. The generator would then consist of 26 cells in order to effectively utilize the 26 volts available from an aircraft power supply, after allowing 2 volts for power conversion to obtain a constant current. It should be noted that the generator could be designed to match virtually any combination of current and voltage by selecting a series and/or parallel combinations of electrochemical cell arrangements.

Substituting the value of $N = 26$ and $W = 0.2 \text{ lb/hr}$ into equation 3 shows that a generator current of 11.7 amps is required. This current and a current density of 35 ASF anticipated with each cell operating at 1.0 yields a calculated electrode area of 0.334 sq. ft. for each of the 26-cells. Based upon previous considerations of the heat and mass transport problems associated with a prototype generator, it was concluded that the preferred cell geometry should be rectangular with the short side being about 4-inches long. These considerations and the availability of a standard O-ring to match the design resulted in a final design point of 33.7 ASF with an effective electrode area of 4.25×11.75 inches (50 sq. inches).

B. Air Feed Requirement

Two-tenths of a pound of oxygen per hour represents a volume flowrate of 2.24 SCFH. Since air contains approximately 21% oxygen, the theoretical flowrate of air required to deliver 0.2 lb O₂/hr is 2.24/0.21 or 10.7 SCFH. It was felt that, during testing air flowrates as high as 5 times this theoretical amount (53.5 SCFH) might be required in order to assure that polarization from inert gas build up would not occur. When oxygen is generated at more or less than 0.2 lb/hr the flowrate of air required increases or decreased accordingly. (See Appendix).

C. Generator Cooling Requirements

Heat is generated during the electrochemical separation of oxygen from air by joule heating of the electrolyte and inefficiencies in the electrode reactions. Such inefficiencies result from polarization losses at the cathode and overvoltage occurring at the anode. This heat causes the generator temperature to rise until the heat generated is balanced by the heat losses. During prior studies at TRW, various methods for removing this heat were considered, including evaporative cooling, coolant circulation through the generator, and conduction to air cooled fins. The later technique was selected as most applicable to a first design because it is a passive system in which the cooling requirements can be separated from other processes occurring in the cells. In this manner, the heat produced inside the generator is transferred to the bi-polar plates and conducted to the outer-edges that make up the cooling fins.

In designing the bi-polar plate, a higher average cell voltage than actually anticipated was assumed. A value of 1.2 volts per cell or a total generator voltage of 31.2 volts was adapted, for a heat load of 31.2 v x 11.7 amps or 364 watts. The heat load for the design point of 26 volts and 11.7 amps is only 304 watts. The increased cooling load assumed in designing the bi-polar plates enables operation of the generator at oxygen outputs above the design point. The cooling air flow requirements for stabilizing the generator's temperature is proportional to the heat (watts) to be removed divided by the temperature rise of the coolant as it flows across the cooling fins. With an air coolant at 70°F at the inlet and 14.7 psia, the constant is 3.16 or

$$\text{Cooling Air Flow, CFM} = \frac{(\text{Heat Load, watts})}{\text{Temp. Rise, } ^\circ\text{F}} \times 3.16$$

The thermal analysis is described in the Appendix along with sample heat transfer calculations. For a heat load of 364 watts and assuming 10°F as the allowable air temperature rise, the cooling flowrate would be 116 CFM.

D. Humidification Requirement

The concentration of the electrolyte inside the concentrator is a direct function of the generator's operating temperature. In order to maintain the concentration at a fixed level the moisture content or dew point of the supply

air, exhaust air, and oxygen must be balanced so that no net transfer of water into or from the generator occurs. This is done to assure that the electrolyte is neither desiccated nor diluted during the course of generator operation.

The following example illustrates the dependency between air feed dew point and KOH electrolyte vapor pressure. Assume that the generator is operating at 100°F and the KOH concentration is 30%. The dew point of the air entering must be of such a value that it matches the vapor pressure of the electrolyte. In Figure 4 the relationship between temperature and electrolyte vapor pressure is shown. At 100°F the vapor pressure of a 30% KOH solution is 28.8 mm of Hg. For the water vapor in the air feed to match this vapor pressure, the dew point of the air must be equal to the temperature at which air would be 100 per cent saturated at a vapor pressure of 28.8 mm of Hg. This temperature is found by reading the abscissa of the point formed by the intersection of the water vapor pressure curve with a horizontal line drawn through the 28.8 mm of Hg ordinate. For the example given the dew point required is 82.3°F. Conversely, if it is known that the cell is at an equilibrium temperature of 100°F and that the dew point of the equilibrium exhaust air is 82.3°F, the concentration of KOH within the generator is 30 per cent. If the air had a dew point greater than 82.3°F it would contain water vapor at a pressure of more than 28.8 mm Hg. This would cause water to condense in the electrolyte and dilute it until the point was reached where the electrolyte vapor pressure matched the vapor pressure of the inlet air. If on the other hand the air entering the generator had a dew point of less than 82.3°F the air would pick up (evaporate) water from the electrolyte thus desiccating it and causing it to become more concentrated. The process would continue until the vapor pressure of the electrolyte matched that corresponding to the air feed dew point.

The design parameters for the 0.2 lb/hr generator are summarized in Table 1.

Generator Fabrication

The basic cell construction consists of two porous metal electrodes separated by a porous matrix which contains the electrolyte. Separating the individual cells in the series are bi-polar plates. These components are shown in Figure 5.

A. Electrodes

The electrodes consist of a porous layer of platinum black and waterproofing agent spread uniformly on and supported by a fine mesh nickel screen. The electrode is flexible and highly resistant to corrosion. Its total thickness, including the coating is 0.0045 inches. The thinness of the electrodes makes the generator light and compact. It also minimizes polarization at the air cathode which is caused by a blanket of inert gases that builds up in the pores of the electrode as oxygen is consumed there. Keeping the electrode thin minimizes the thickness of the inert gas blanket, thus allowing oxygen to diffuse easily to the reaction zone.

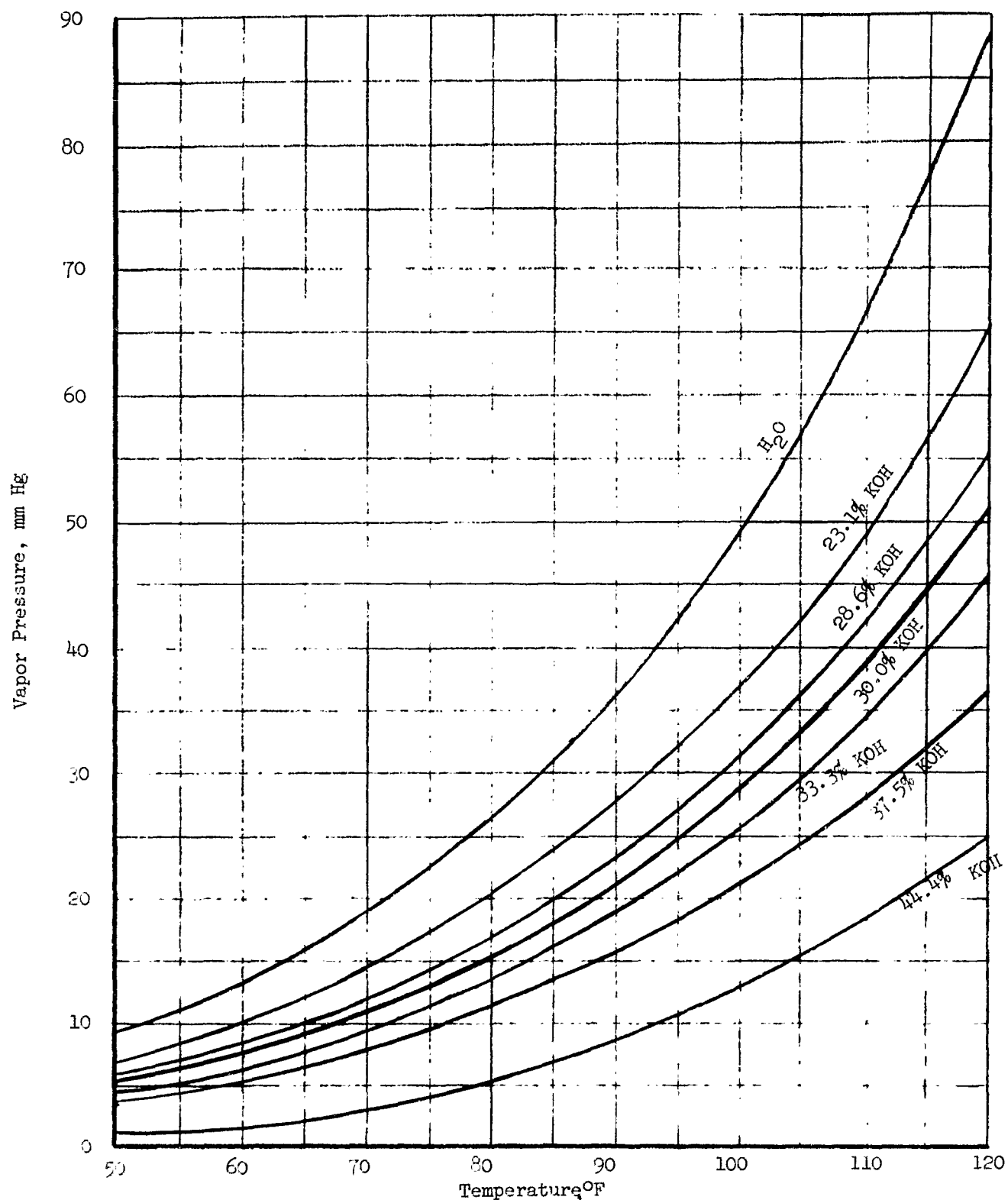


FIGURE 4
TEMPERATURE VERSUS VAPOR PRESSURE OF KOH SOLUTIONS

Table 1. 0.2 lb/hr Oxygen Generator Design Parameters

Effective Electrode Area, ft ²	0.347 (4.25 x 11.75 in)
Current Density, ASF	33.7
Current, Amps	11.7
No. Cells, Series Connected	26
Generator Voltage, volts	26
Voltage Per Cell, volts	1.0
Air Feed Flow Rate, SCFM	
Theoretical	0.178
2 x Theoretical	0.356
3 x Theoretical	0.534
4 x Theoretical	0.715
5 x Theoretical	0.892
Generator Temperature, °F	100
Air Pressure, psia	15.5 decreasing to 6.5
Cooling Air Flow Rate, SCFM	96
Electrolyte Concentration, %KOH	32
Air Feed Dew Point, °F	80

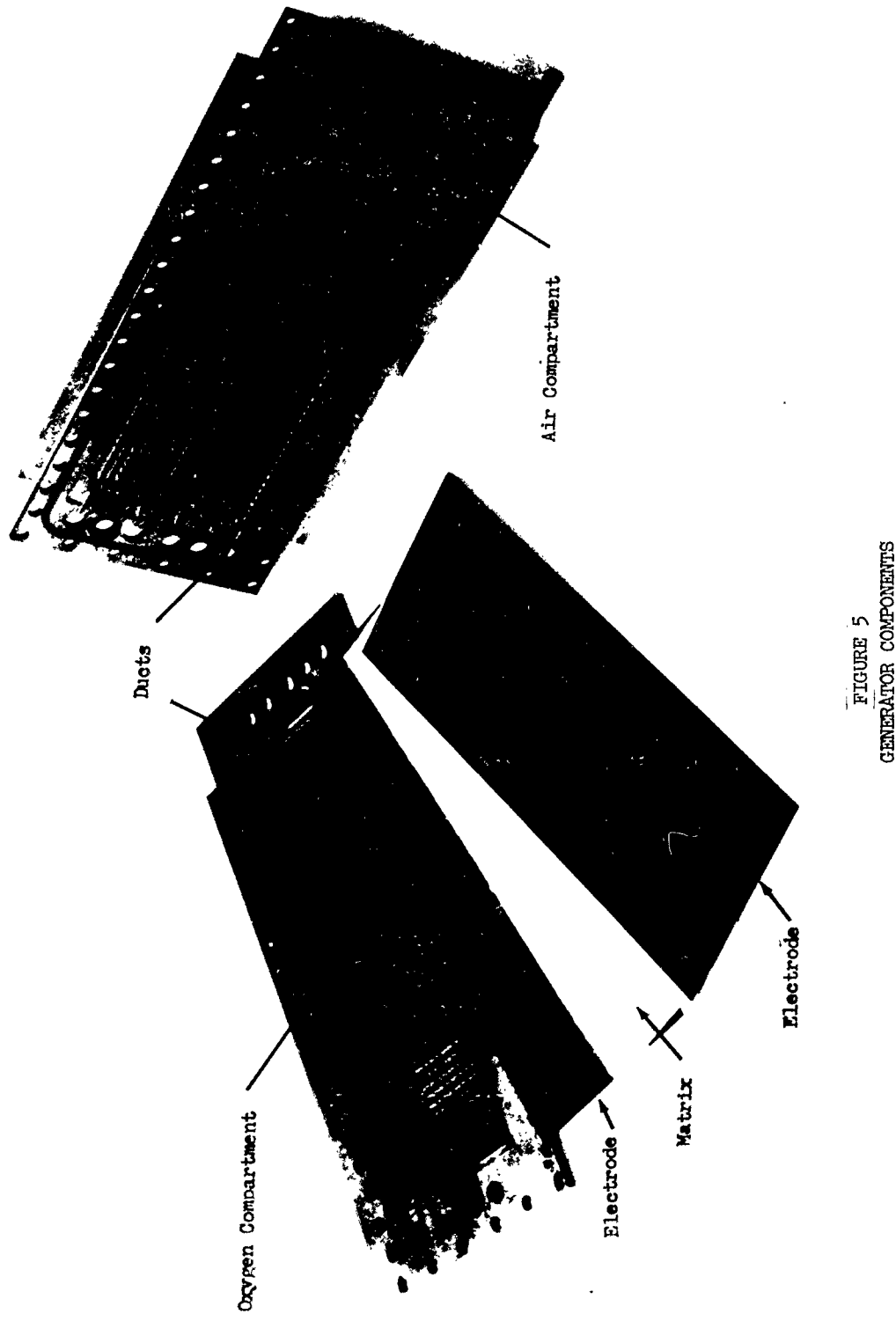


FIGURE 5
GENERATOR COMPONENTS

B. Electrolyte Holding Matrix

The porous matrix used to contain the electrolyte between the cell electrodes is a high purity form of asbestos. It provides a uniform separation of the electrodes and was designed to hold the electrolyte in proper contact with the electrodes regardless of their orientation relative to the external forces of gravity or acceleration. The matrix also serves to separate the air compartment gases from the oxygen compartment. Close spacing effectively lowers the cell internal resistance and prevents air from diffusing through and mixing with the evolved oxygen on the anode side. A matrix thickness of 0.03 inches was used in the generator assembly.

C. Electrolyte

After assembly, the matrix and electrodes were filled with electrolyte solution. Although cells have been operated with acid and neutral electrolytes, performance has been found to be better with an alkaline electrolyte. Potassium hydroxide is the specific electrolyte selected, because its aqueous solutions have a high electrolytic conductance. The electrolyte concentration used was 32 per cent by weight.

D. Bi-Polar Plates

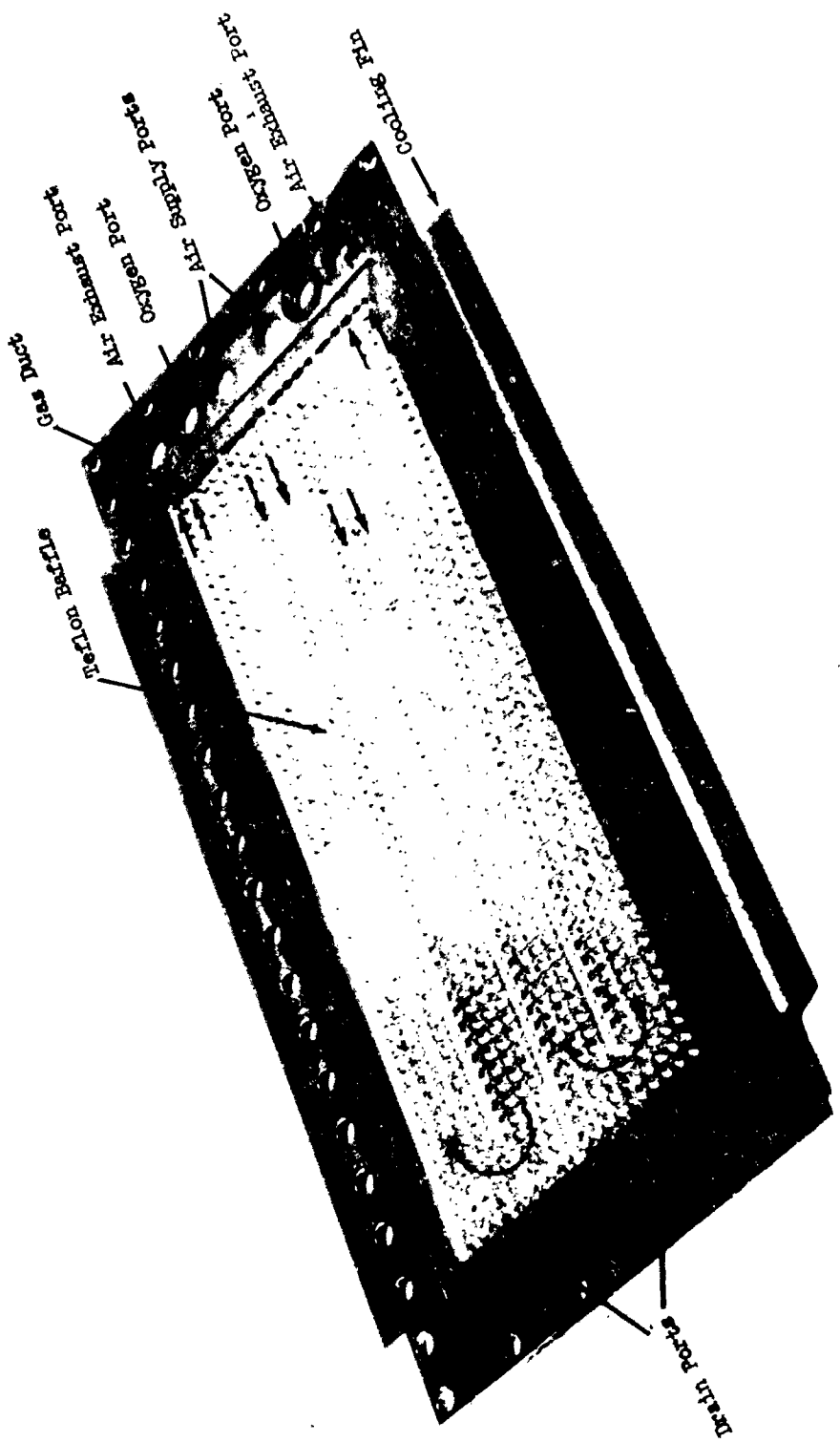
The bi-polar plates were fabricated from a magnesium alloy. Following machining of the plate it was plated first with nickel and then gold to prevent corrosion. The bi-polar plate serves several functions; it supports the electrodes and electrically connects individual cells in series; it serves to manifold the air effectively to the surface of the electrodes; and its cooling fins provide the means of removing waste heat produced in the cells. Photographs of the air and oxygen sides of the bi-polar plate are shown in Figures 6 and 7, respectively. A recessed area on the air side is used to retain the electrolyte matrix. The baffles used to direct the gases are lengths of Teflon spaghetti tubing inserted between closely spaced pins machined into the plate. The O-ring arrangement, ports, and gas ducting can also be seen in the photograph.

Air is distributed to the individual cell air compartments down the two ports in the center at one end of the bi-polar plate. The air then passes laterally through the ducts, indicated in Figure 6, into the gas compartments. After passing over the electrode surface, the waste gases pass out of the ducts and down the two ports to the outside of the bi-polar plate. The gas ducting and ports were designed according to the technique presented in the Appendix.

The oxygen compartment had two ports although one is plugged at the end plate. The extra port was added so that the air and oxygen compartments could be interchanged. The oxygen generated on the anode passes out of the oxygen compartment as indicated by the arrows in Figure 7.

After fabricating the bi-polar plates for the 2- and 4-cell units, a new technique was developed to cut down the fabrication time required and at the same time improve the design. Fabrication of the bi-polar plate initially required that 18 slots from the gas ports to the gas compartments be machined

FIGURE 6
AIR COMPARTMENT OF BI-POLAR PLATE



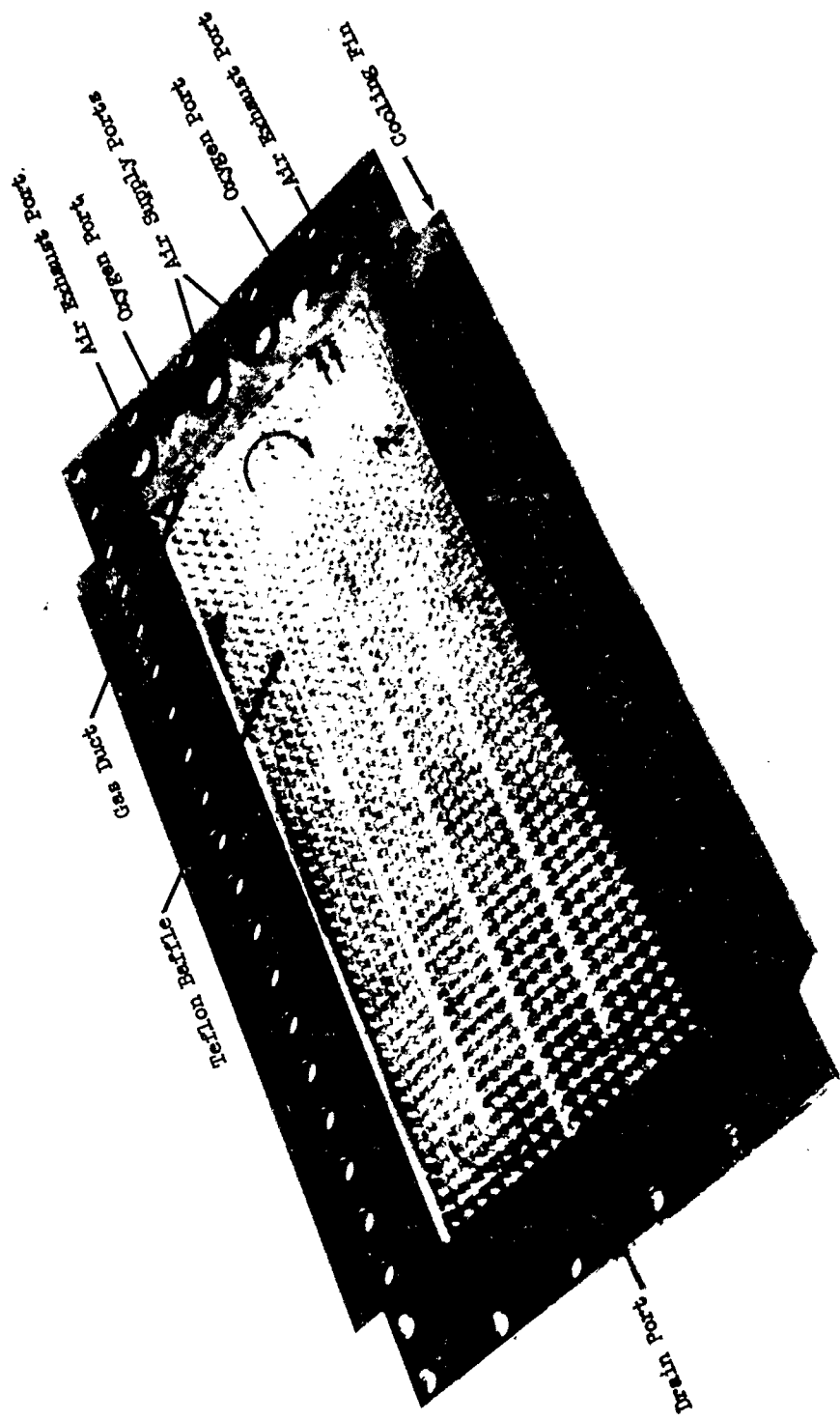


FIGURE 7
OXYGEN COMPARTMENT OF BI-POLAR PLATE

into each plate. After the bi-polar plate was nickel plated, a stainless steel tube was manually inserted into each of the machined slots. Silicone rubber was then used to fill the voids that remained after putting the round tube in a rectangular slot. The new technique involved drilling the ducts directly into the bi-polar plate, with special flexible drills. In all aspects the drilled ducts were far superior to the manually inserted ones.

E. Edge Sealing

The cells are sealed when the smooth flange area of the bi-polar plates are pressed tightly against the wet matrix. The rubber gasket frames the matrix and serves to control the matrix compression. It also prevent direct electrical contact between the flanges of the bi-polar plates which would short out the cells. The initial generator design called for a 10 mil epoxy coating on the outer edge of the bi-polar plate rather than the gasket, but difficulties were encountered in applying such a thin coat of epoxy. A 15 mil gasket thickness had to be used since 10 mil neoprene was not available. As will be noted later, this substitution decreased the extent to which pressure differentials between gas compartments could be tolerated. Rubber O-rings were used to seal the generator from external leaks. O-rings were also used to seal the ports in the bi-polar plates, which when assembled in the 26-cell module formed the internal manifolds for the gases.

F. End-Plates

The series stack of 26 individual cells were sandwiched between two structural end-plates as shown in Figure 8. Drilled and tapped holes in the end-plates permitted ready coupling to the external gas systems through standard fittings. The end-plates were bolted together to seal the assembly. One end-plate was machined to serve as an air compartment while the other served as an oxygen compartment. A photograph of the actual 26-cell model is shown in Figure 9.

Auxiliaries and Instrumentation

A photograph of the concentrator and test rig delivered under the contract is shown in Figure 10. As seen by the schematic diagram in Figure 11, the oxygen concentrating system auxiliaries are composed of the air supply, air exhaust, oxygen exhaust, temperature control, and power supply subsystems.

A. Air Supply Subsystem

Compressed air was used as the source of air fed to the generator except during operation at less than atmospheric pressure. Tests at reduced pressures were carried out by using a positive displacement carbon vane pump. The desired vacuum was simultaneously drawn on both the oxygen and air sides. The air flowrates were maintained by regulating the leakage through the inlet air flow control valves. Acting as a compressor, the pump has the capacity to deliver 2.7 SCFM against a pressure head of 10 psig. This pump, therefore, could also be used as the air source for the generator.

A MSC100LEC Pall Trinty filter was used to remove foreign particles from the incoming air stream, and a soda lime canister was used to absorb the small amount of carbon dioxide found in air to prevent the CO₂ from neutralizing the KOH electrolyte.

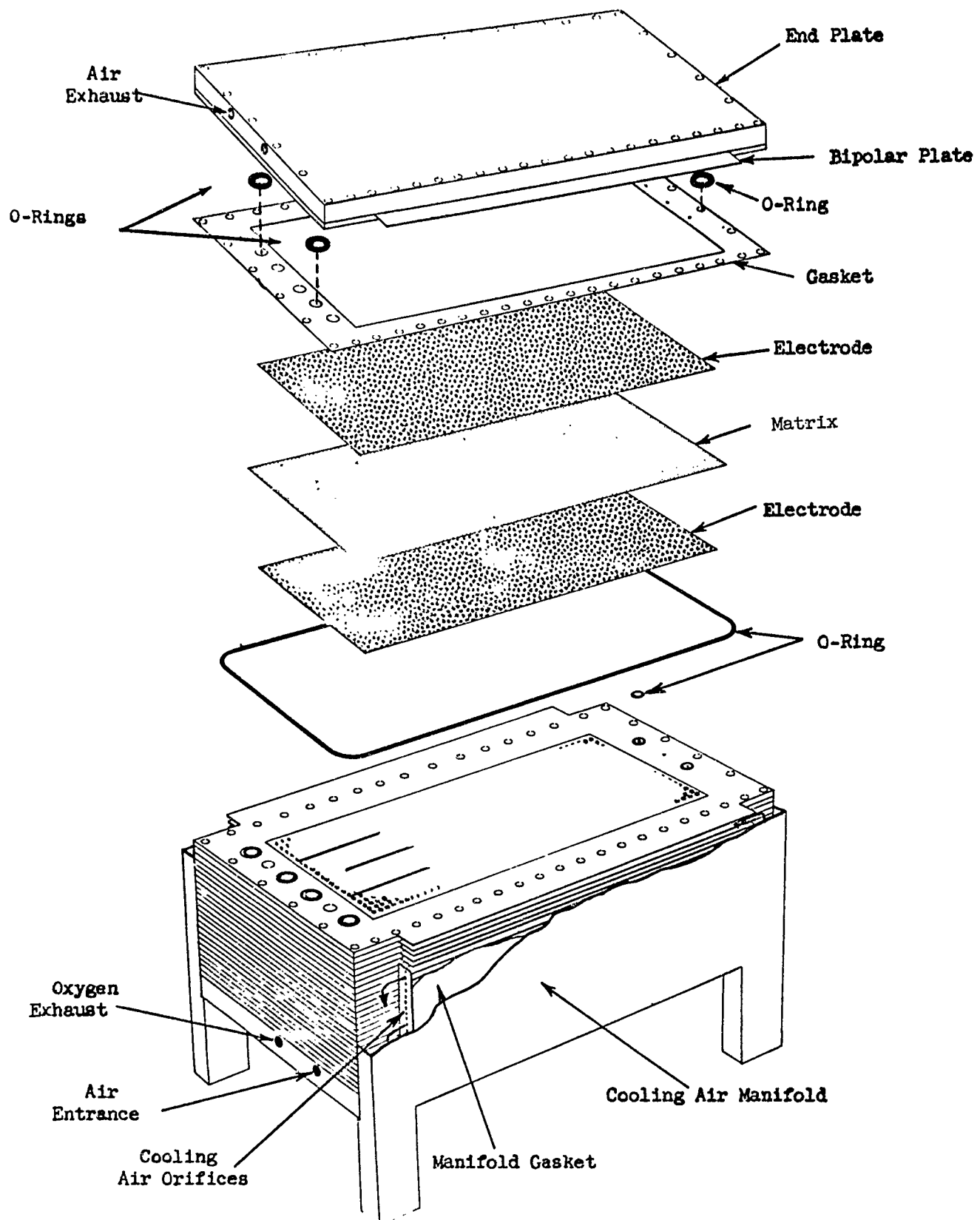
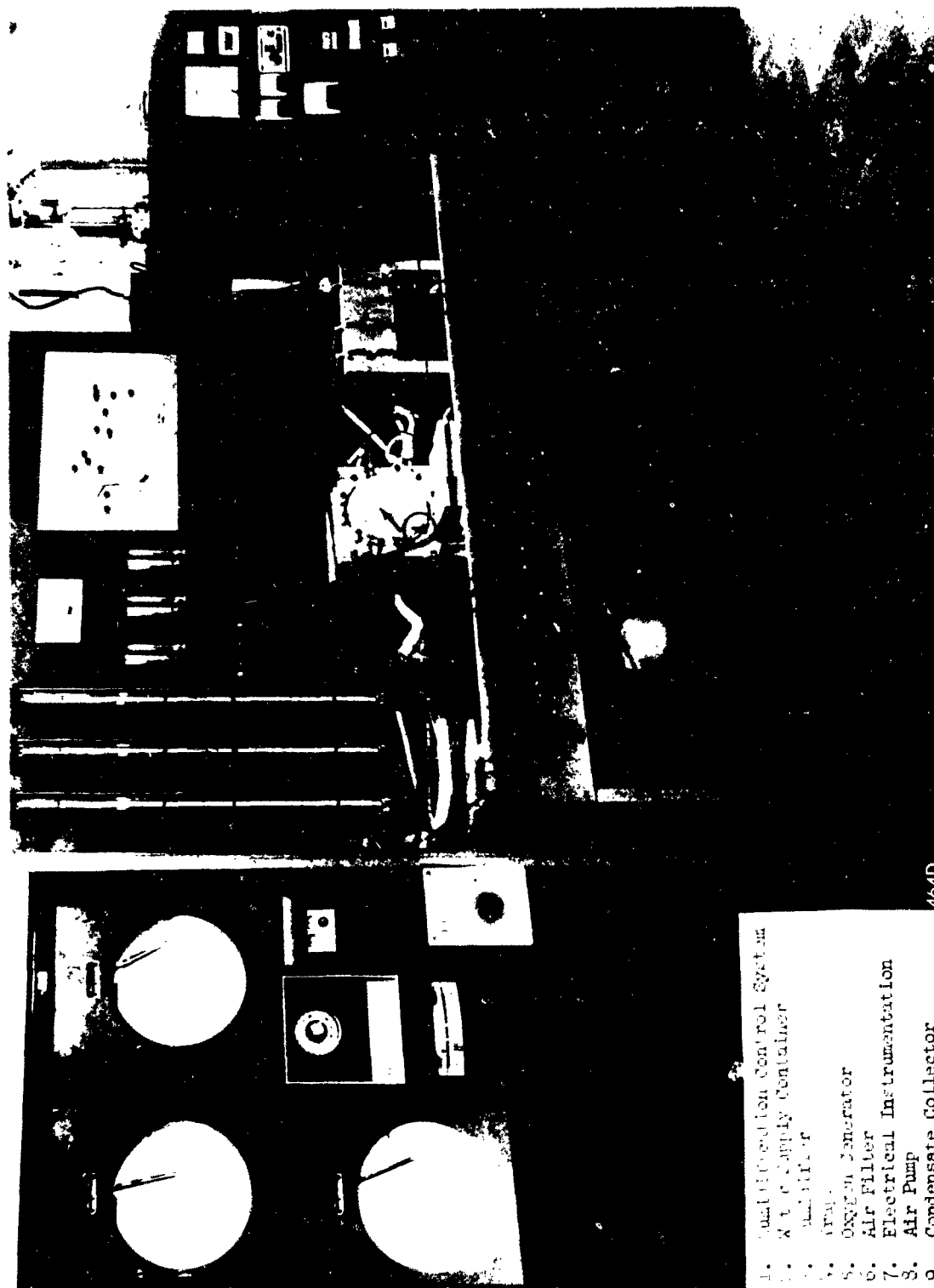


FIGURE 8
TWENTY-SIX-CELL ASSEMBLY



FIGURE 9
TWENTY-SIX-CELL OXYGEN GENERATOR



464D

1. Control Operation Control System
2. Water Supply Container
3. Pump
4. Oxygen Generator
5. Air Filter
6. Electrical Instrumentation
7. Air Pump
8. Condensate Collector

FIGURE 10
GENERATOR AND CONTROL SYSTEM

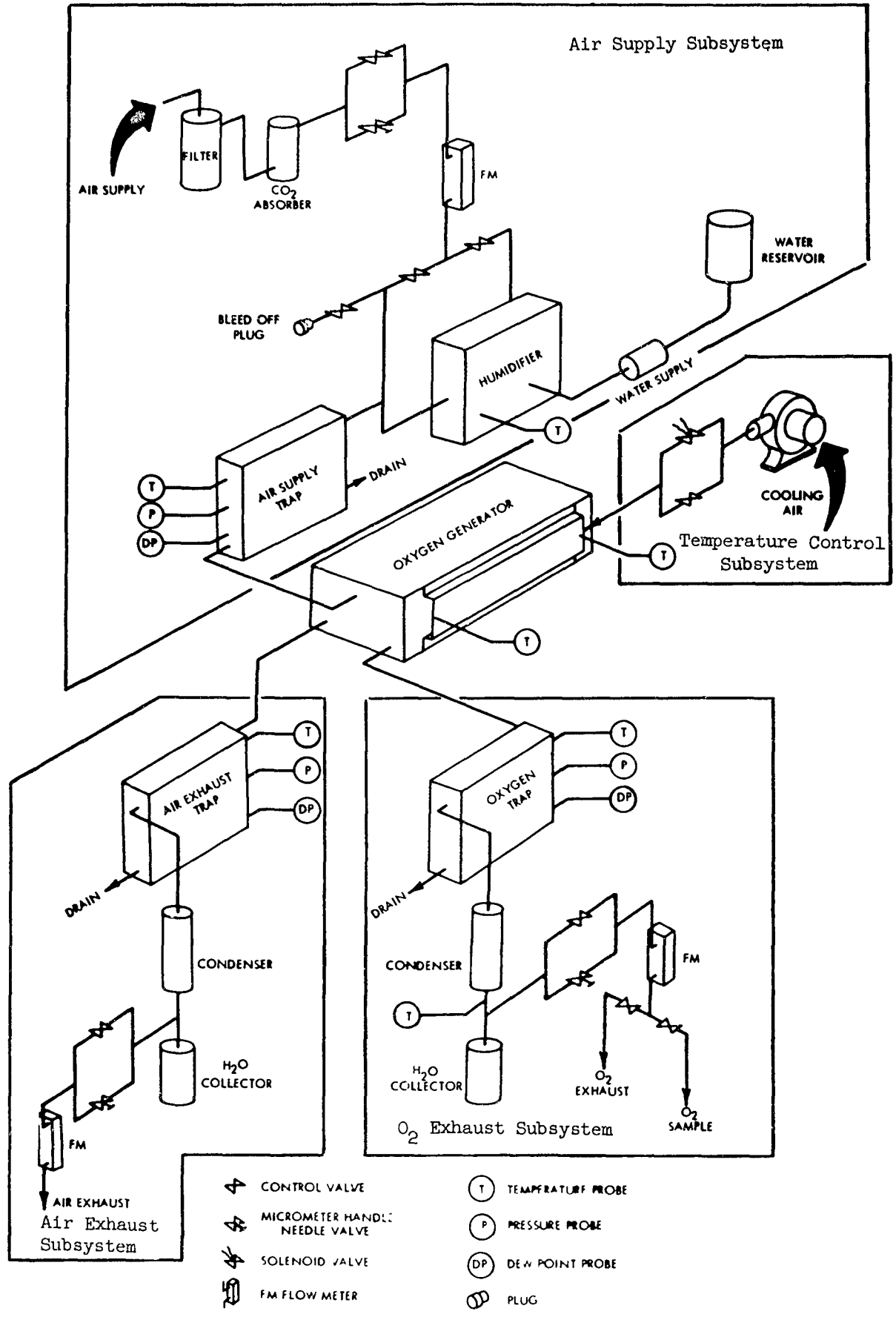


FIGURE 11 TEST RIG SCHEMATIC

Although standard off-the-shelf items were used for the system auxiliaries wherever possible, such was not so with the humidifier. Commercial humidifiers would have required extensive modifications and conventional laboratory humidifiers would not have contributed the type of information important to the ultimate prototype system development. Therefore, a humidifier was designed with the capability of providing information essential to later phases of the generator development.

The humidifier was made to operate according to wicking principles. The humidifier capacity could easily be increased or decreased by adding or subtracting segments to the basic unit. Each segment consisted of two 20 mil thick Dacron felt wicks between which was sandwiched a 3 mil thick sheet of aluminum foil. The foil transfers heat from the humidifier heaters. An internal heater consisting of a 50 watt wire wound resistor and an external heating tape provide the heat to overcome the cooling associated with the evaporation of water. The frame and the humidifier end-plates were fabricated from Plexiglas. A sketch of the unit is shown in Figure 12.

Each wick obtains its water from a water absorbent paper pulp material. The absorbent material is supplied, in turn, through a transport wick from a water supply container. The transport wick is a folded strip of 50 mil thick Dacron felt. The choice of water wicking and water absorbent materials was based upon a material evaluation program sponsored by the Air Force under Contract AF 33(616)-8159.

Air is humidified by passing it over the wick surfaces. Each frame has an inlet and exit port. When the humidifier cells are assembled as a unit, these ports form the air manifold passages. Uniform air distribution between the various air compartments results from making the pressure drop through the individual ducts leading to the air compartment 100 times the pressure drop of the air passing through the manifold. Calculations used to design the humidifier ports and ducts are presented in Section VIII.

In order to operate the humidifier for long time periods during unattended operation, a water reservoir is employed. As water is used by the humidifier, more is transported to it from the water supply container, see Figure 13. The water removed from the supply container was replaced, in turn, from the large reservoir. The capacity of the system is sufficient to permit over 60 hours of continuous test rig operation under the generator design conditions.

Between the humidifier and the generator was located a moisture trap to prevent any entrained water from being carried over from the humidifier to the generator. This moisture trap is discussed in more detail on page 33.

B. Air and Oxygen Exhaust Subsystems

The air and oxygen subsystems are illustrated in the lower portion of Figure 11. Each of the exhaust lines contains a water cooled condenser to remove water vapor contained in the gas stream. The temperature of the oxygen is maintained at $70^{\circ}\text{F} \pm 5^{\circ}$. Entrainment moisture traps were located at the air and oxygen exhaust ports to prevent any liquid carry over from damaging other components in the system.

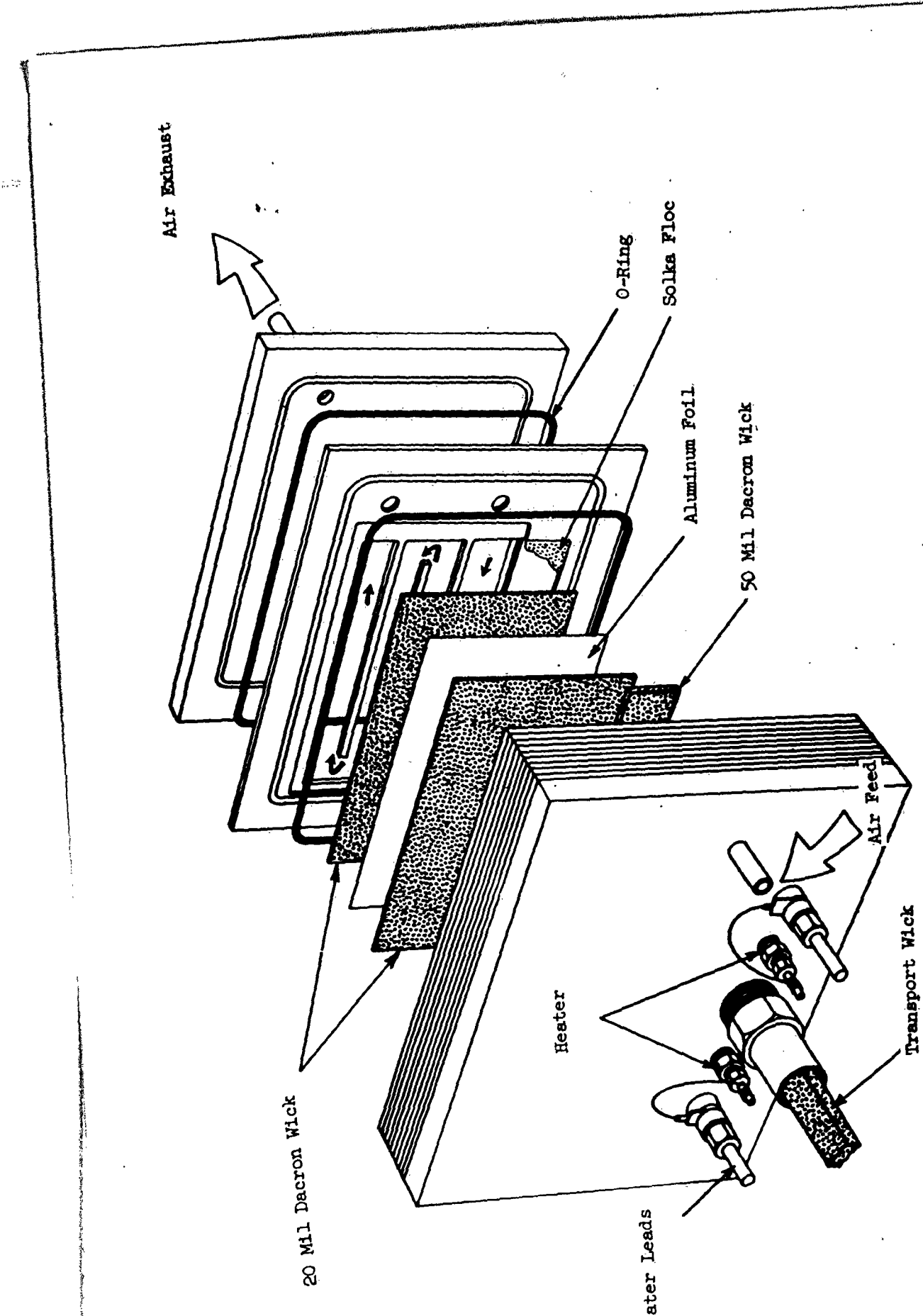


FIGURE 12
HUMIDIFIER ASSEMBLY

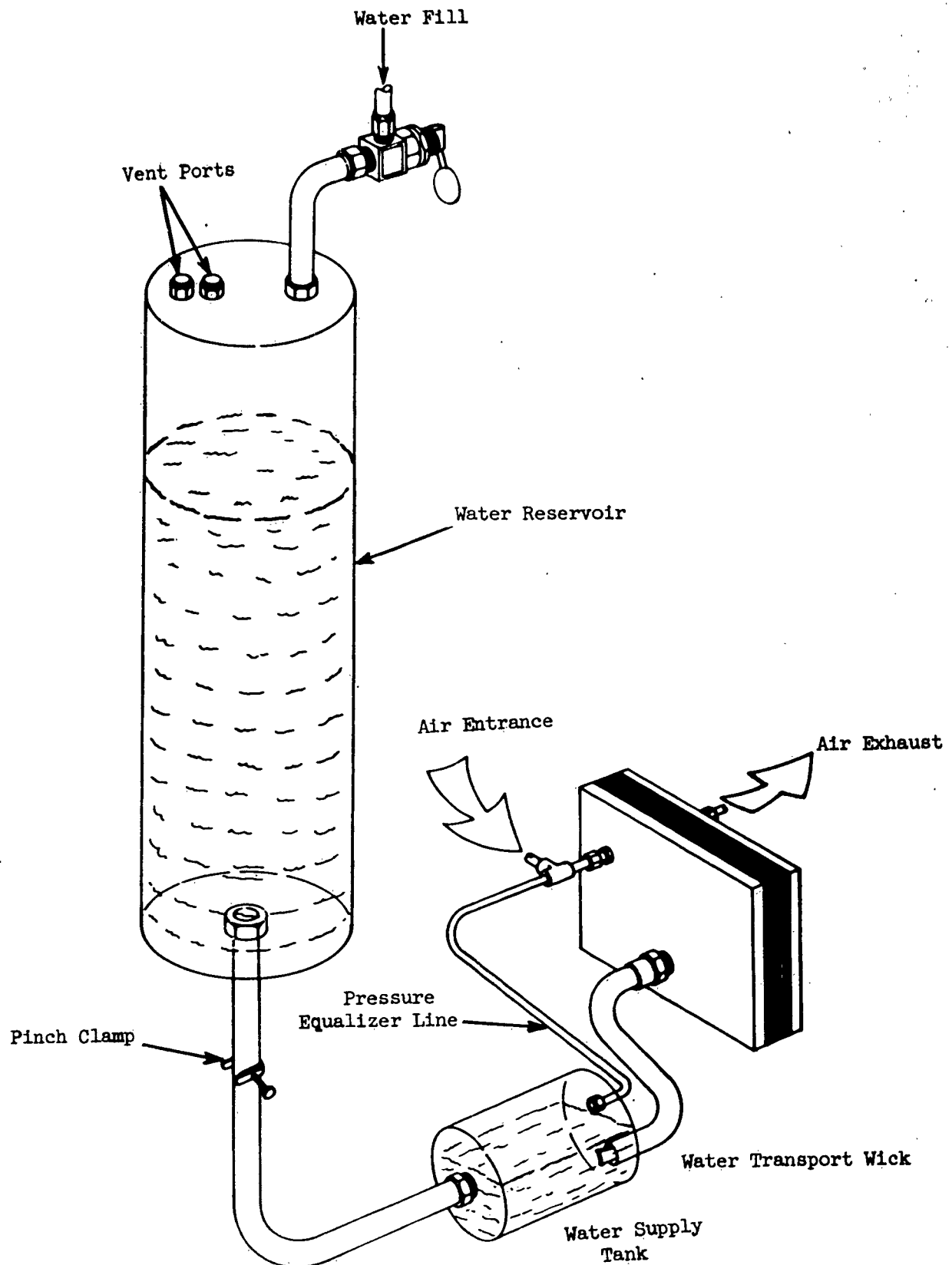


FIGURE 13
WATER FEED SYSTEM

C. Temperature Control Subsystem

Normally an air blower would be used to supply air to meet the cooling requirements; however cooling air from a laboratory air line was used during the testing. A solenoid valve, connected in parallel with a hand throttling valve controls the cooling air flow. The solenoid is activated by the temperature controller which senses the cell temperature by means of a thermocouple located on a bi-polar plate fin.

The cooling air divides into two flow paths, one-half of the air passing over one set of fins and the other half over the fins on the opposite side. The air is passed through a channel that opens into the cooling fin passageways, (see Figure 8). At the exit is located a plastic strip with a series of orifices which line up with the center of each fin passage. The pressure drop across the orifice is roughly 100 times the pressure drop along the fin passageway, with the result that the air is distributed uniformly through each of the fin channels. Calculations used to design the coolant passage dimensions are presented in Section VIII.

D. Power Supply Subsystem

A commercial power supply capable of delivering 0 to 36 volts DC output at 0 to 15 amps was used as a substitute for the standard 28 volt DC aircraft power supply. The model provided with the unit has a capability of being either a constant current or a constant voltage source.

Test Rig Instrumentation

Since the delivered piece of hardware was to be a laboratory model, it was essential that adequate instrumentation be supplied to measure and control various operating parameters. In designing the instrumentation, the controls were made as simple and reliable as possible.

The instrumentation can be grouped under the following headings: Gas Flow and Pressure Control, Electrical Measurements, Temperature Monitoring, and Humidification Control.

A. Gas Flow and Pressure Control

Figure 14 is a photograph of that part of the test rig upon which the flow control valves, flow meters, and manometers are mounted. It also shows positioning of the humidifier moisture traps, and generator.

A plug valve in parallel with a micrometer handle needle valve was used to accurately control the flowrates with minimal pressure drops. The plug valve provides coarse flow control and the needle valve provides fine control. Through this valve combination it was possible to accurately control the

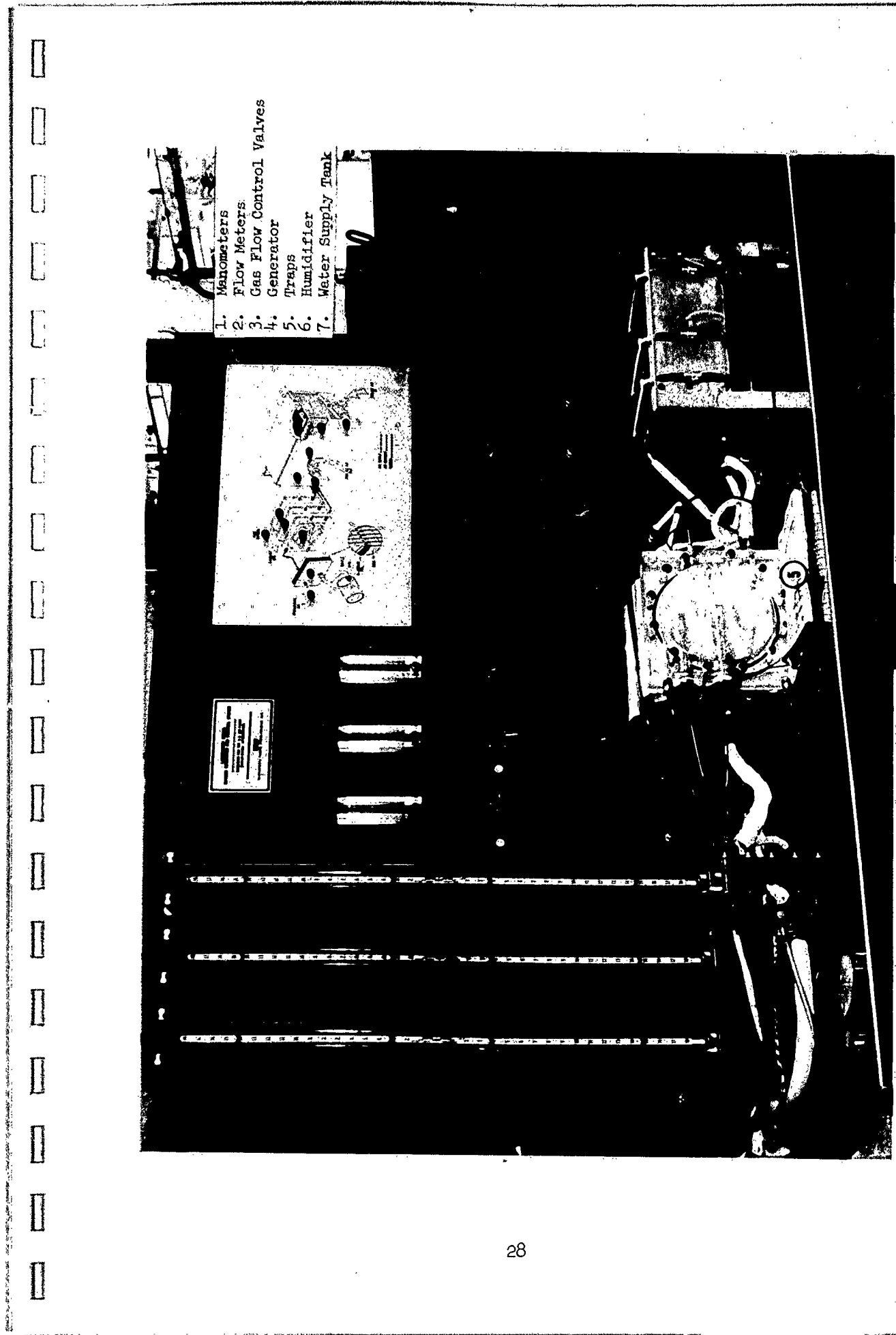


FIGURE 14
FLOW AND PRESSURE CONTROL PANEL

pressure in the air and oxygen gas compartments and the pressure differential between them. The pressure is measured with manometers filled with mercury or manometer fluid, depending upon the pressure range employed in the tests under way at the time. Conventional flow meters are used to monitor the flowrates.

B. Electrical Measurements

As shown in Figure 15, the test rig has instruments to measure current, time and voltage. An accurate ammeter covering the range 0 to 15 amps indicates the current load, hence the instantaneous oxygen output. An amp-hour meter is wired so as to be turned on whenever the generator power supply is operating. The continuous record of the amp-hours gives an exact indication of the total accumulation of oxygen generated by the unit, since it was first turned on.

Two timers are provided. One timer, wired in series with the amp-hour meter and the power supply, keeps track of the total operating time on the generator. By dividing the total amp hours by the total time one obtains the average current (oxygen output) flowing through the generator. The second timer with a reset is used to time individual experiments.

A multi-range voltmeter with a selector switch enables the operator to monitor the voltage across the concentrator, groups of concentrator cells, and the 26 individual cells. The selector switch is wired so that the voltmeter range is automatically changed when switching from individual cell readings to group cell readings. This protects the voltmeter against accidental damage due to overloading.

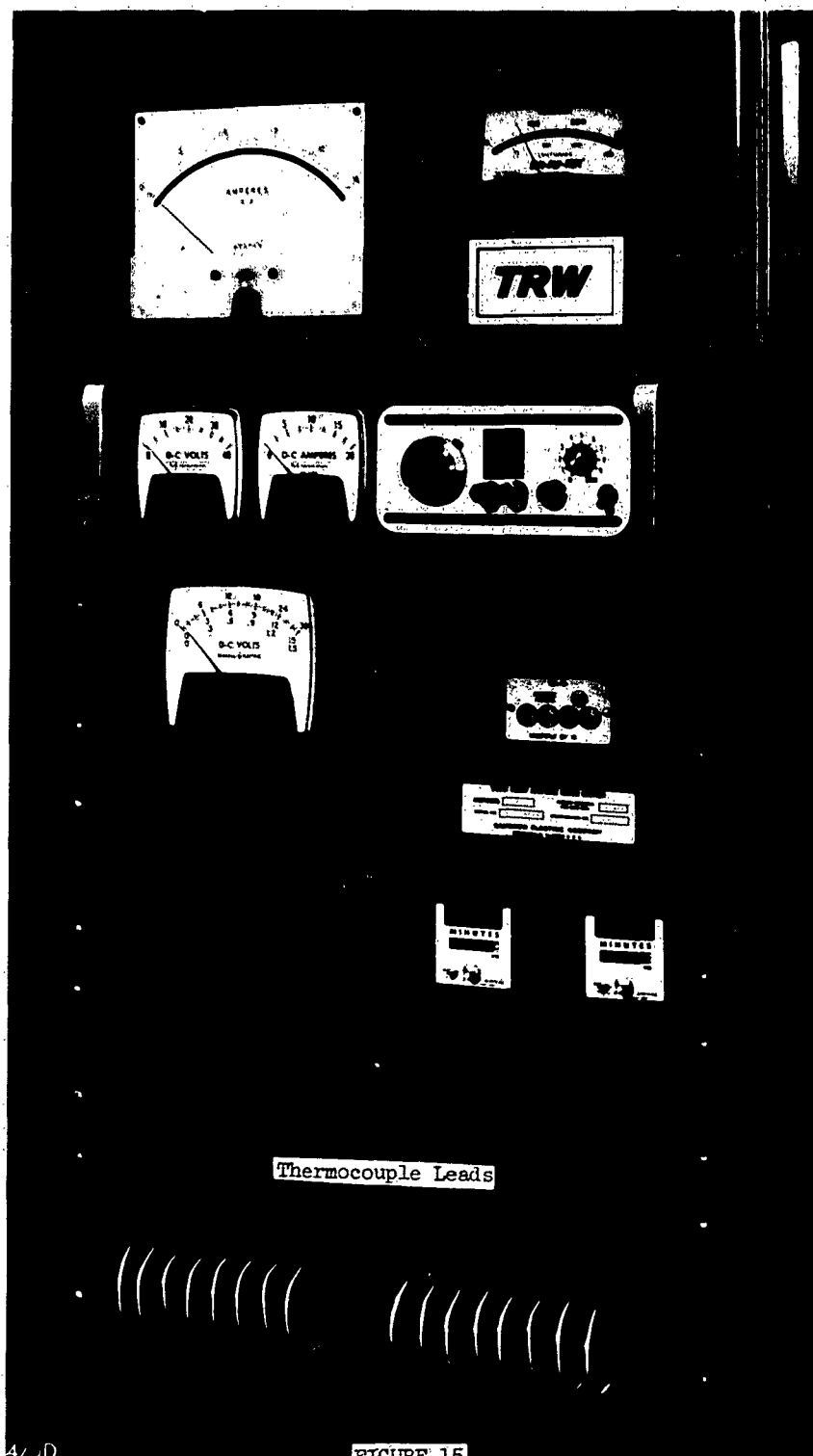
C. Humidification-Temperature Control and Monitoring

A photograph of the heat and humidity control instruments is shown in Figure 16. Instrumentation is capable of recording the dew points of the air feed, air exhaust, and oxygen, and of monitoring the exit air temperature. It also controls the dew point and temperature of the air feed. Other instrumentation on the panel includes the generator temperature controller (T2) and a temperature limit switch (T1) that shuts down the test system in the event that the generator overheats. Both T1 and T2 receive signals from thermocouples located on a cooling fin.

Two temperature monitoring circuits are provided on the panel shown in Figure 15. One circuit monitors 16 iron-constantan thermocouples located within the system. A second circuit, equipped to handle 20 thermocouples is included for a future thermal analysis of the generator heat transfer mechanism. The temperatures can be read from the panel mounted pyrometer although extensions are also supplied for connection to a multi-point temperature recorder.

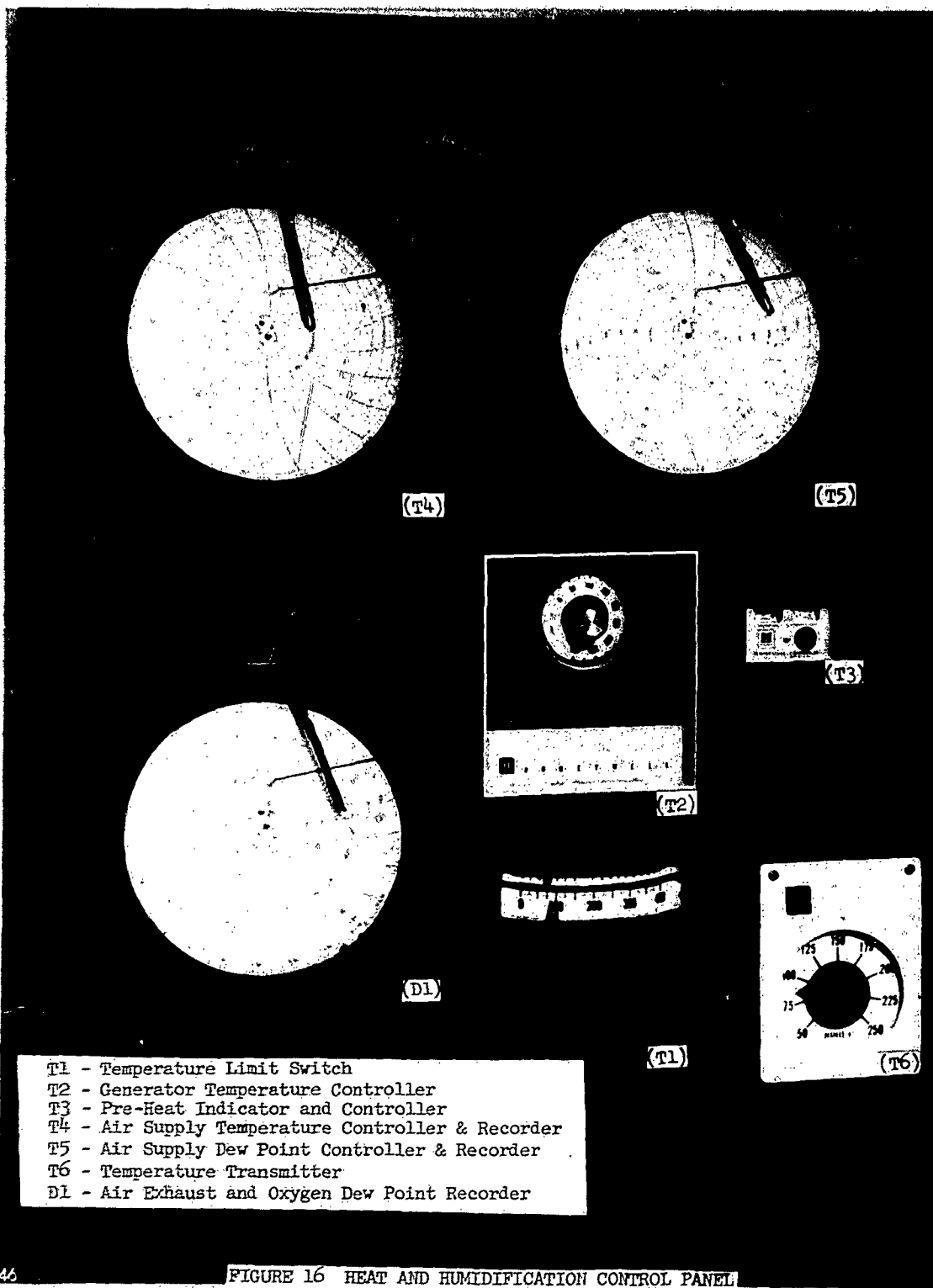
A schematic diagram of the humidification-thermal control and monitoring system is given in Figure 17. It was designed so that the temperature and humidity of the air feed would meet conditions required by the generator electrolyte during start-up and at the desired operating conditions. A temperature transmitter (T6) senses the generator air exhaust temperature. This temperature reflects the generator operating temperature. A pressure signal proportional to the sensed

(a) Numbers in parenthesis refer to the number used on the control panel shown in Figure 16



470D

FIGURE 15
ELECTRICAL INSTRUMENTATION PANEL



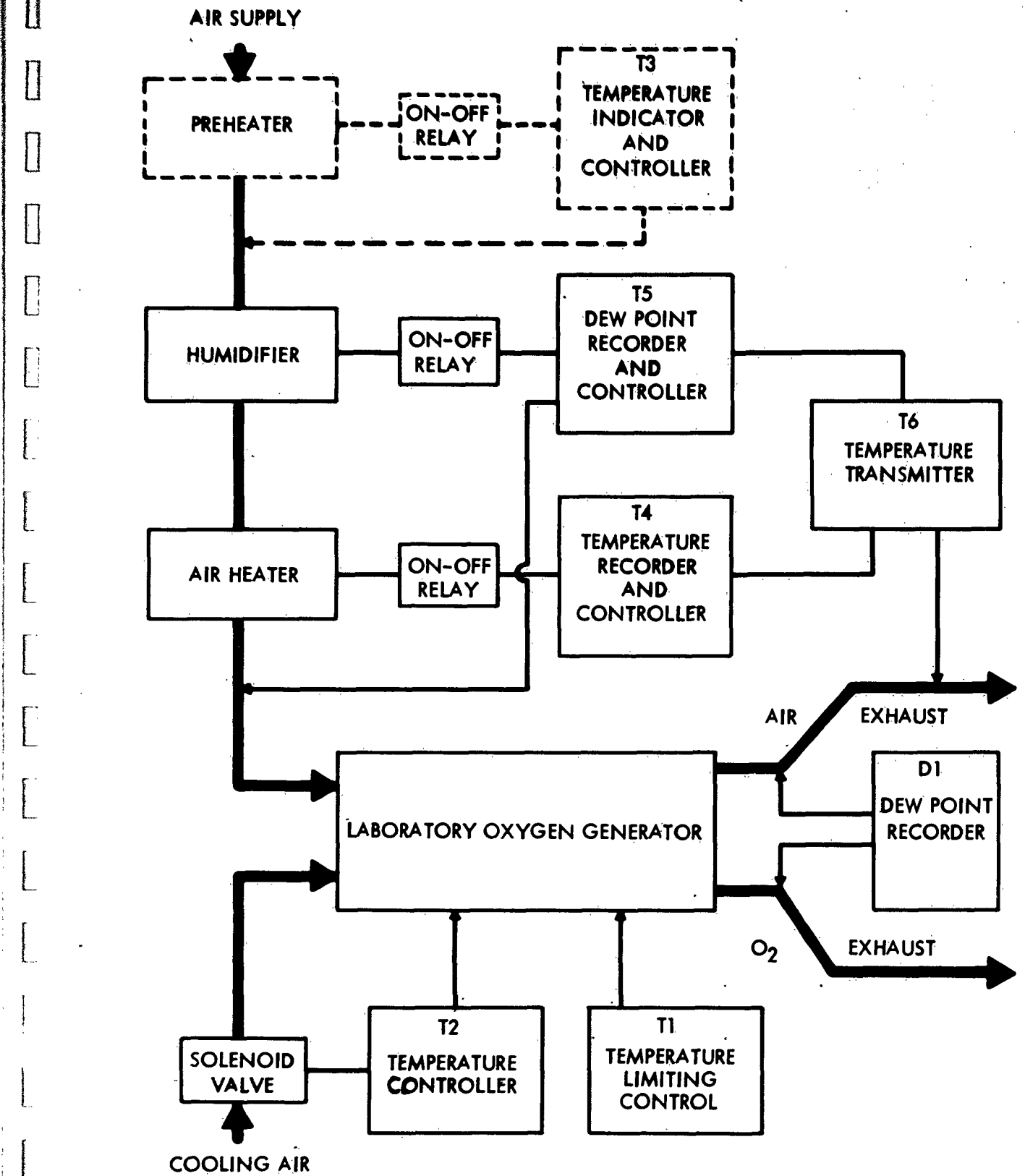


FIGURE 17 HUMIDITY AND TEMPERATURE CONTROL

temperature is then transmitted to the air supply dew point controller and recorder (T2) and to the air supply temperature controller and recorder (T4) which are adjusted so that the air pressure signal received causes their pneumatic control mechanisms to actuate the humidifier heater and the air feed heater, respectively. The relationship between the pressure signal resulting from the air exhaust temperature and the desired dew point and temperature of the air feed can be preset to match the required conditions shown in the temperature versus KOH vapor pressure plot, (Figure 4).

During initial designing of the control system it was felt that one might want to preheat the air feed prior to its entering the humidifier so as to decrease the power required by the humidifier heaters. In the event such a process was used, it would be necessary to have both a preheater and a re heater temperature controller; however the wicking humidification system was found to perform adequately without preheating the air feed and the control pre heat controller (T3) was not used. It is therefore represented in Figure 17 in a dotted form to indicate it was included but not necessary.

A moisture trap located in each of the gas lines immediately adjacent to the concentrator, see Figure 11, in addition to serving as a trap for possible condensation in gas lines, also contains a dew point probe and thermocouple connected to the temperature readout thermometer. Location of the traps in the system can be seen in Figure 14. A detailed sketch of the air supply trap is shown in Figure 18. The dew point probes can be damaged by contact with a liquid (water or KOH solution), and the baffling arrangement built into the traps for catching condensate serves to protect the probes from this hazard. Drain ports were provided to remove liquid carryover. The sensor for the temperature controller (T4) is also located inside the air supply trap. The signal from the sensor activates the controller which powers a heating tape wrapped around the traps and a 4-foot length of copper tubing through which the generator supply air passes prior to entering the air inlet trap. This tape warms the gas to the generator operating temperature.

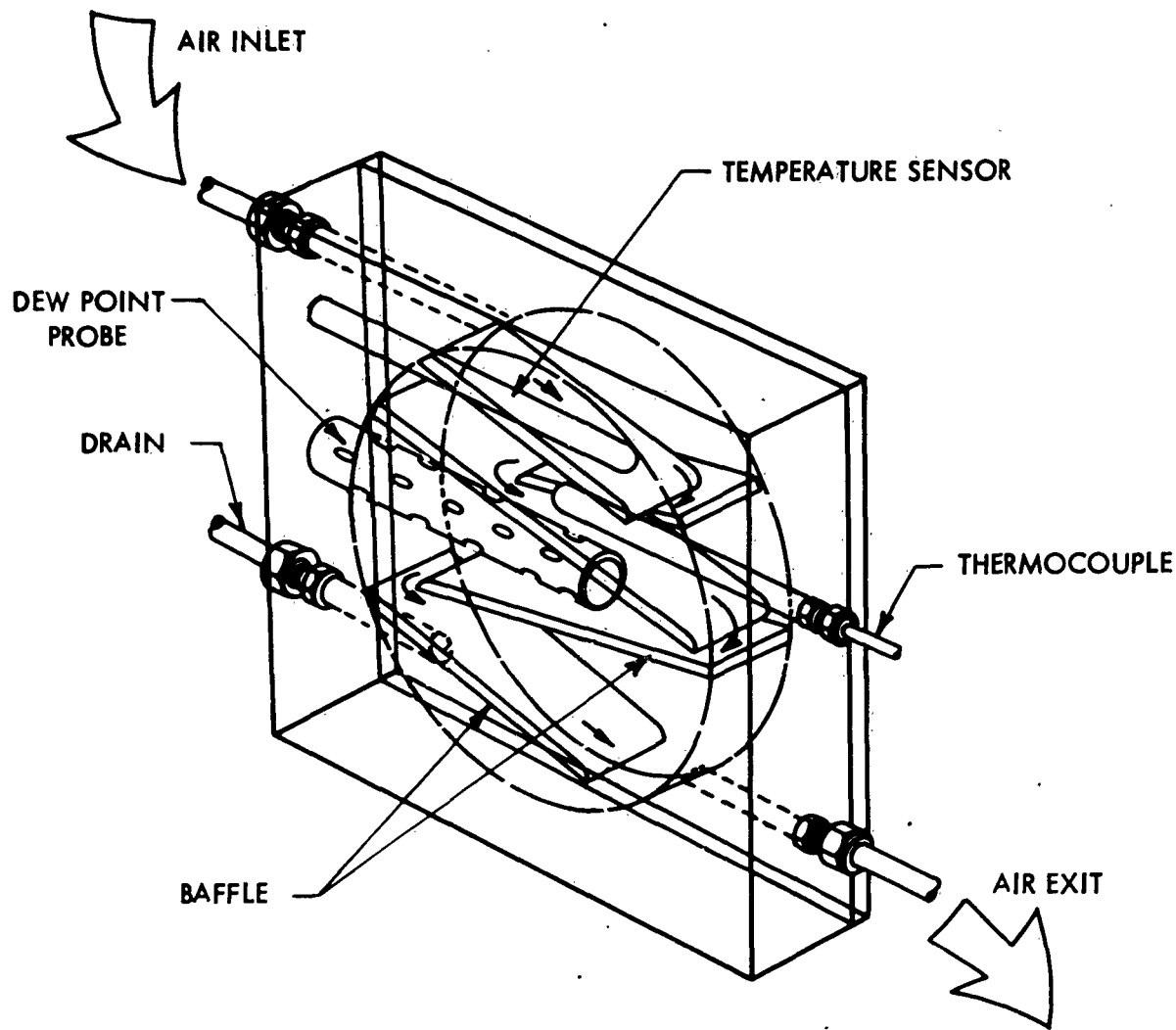


FIGURE 18
AIR SUPPLY TRAP

SECTION IV. EXPERIMENTAL RESULTS

Two and Four-Cell Units

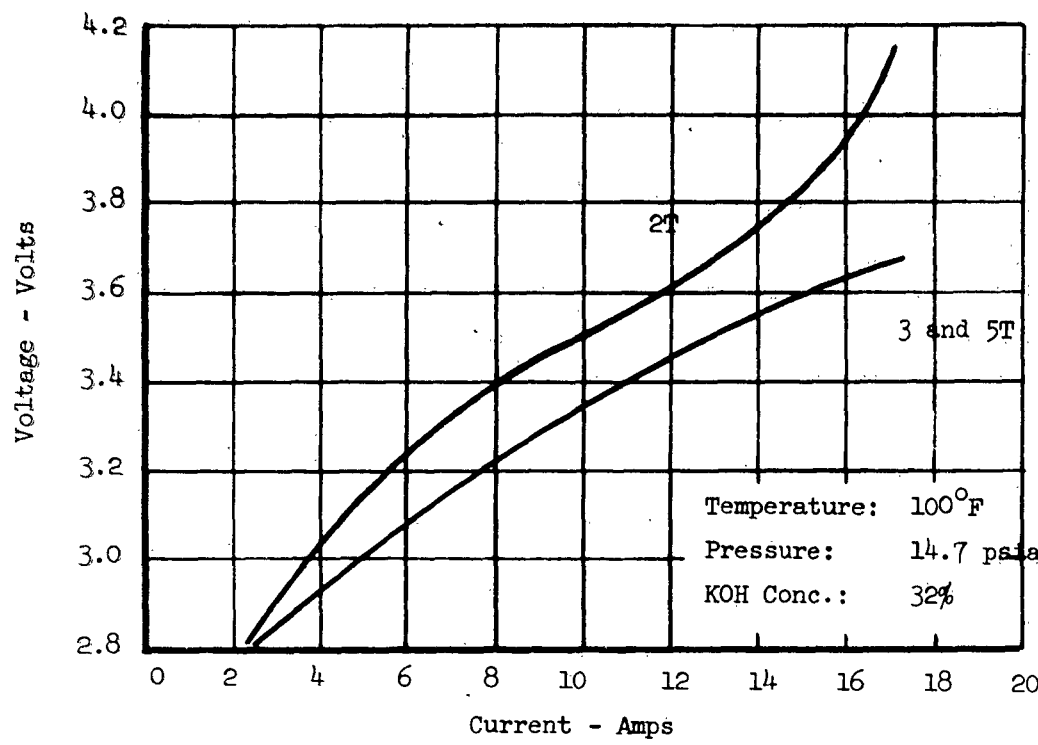
Prior to fabrication of a 26-cell generator, 2- and 4-cell units were built and tested. The 2-cell unit was operated long enough to demonstrate that the manifolding system was adequate and that the generator was performing as designed. No unexpected complications in the concept or initial design were encountered in scaling up prior technology on the smaller single cells to a 2-cell unit having 40% larger electrodes.

Operation of the 4-cell unit further verified the design concept and demonstrated that the control system functioned properly. Initially it was anticipated that operating time on the 4-cell unit would be limited to 24 hours. However, the generator performance was better than designed with a voltage of 3.2 volts at 11.7 amps being typical rather than the expected 4.0 volts (1.0 volt/cell) at the 11.7 current level.

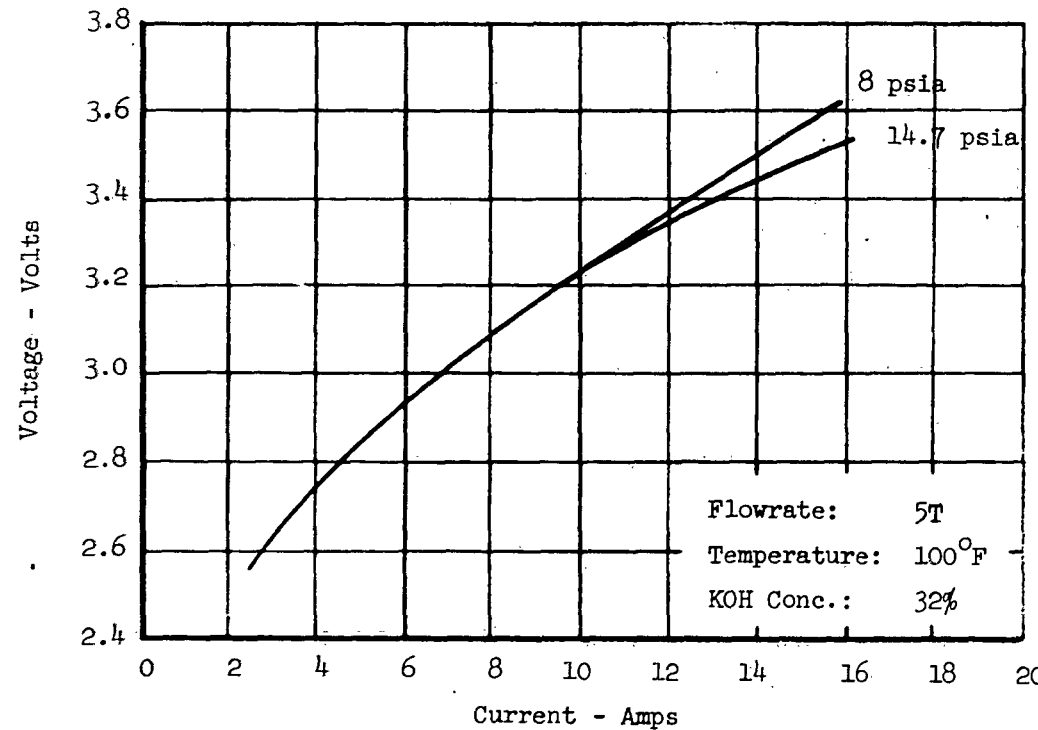
As a result of the improved performance it was decided to continue the testing. After 203 hours the solenoid valve controlling the cooling air failed to open. As a result, no cooling air passed over the fins. Within 3 hours the generator temperature reached 120°F, and the high temperature limit switch shut off the generator and appropriate test rig power.

Rather than continue with the test it was decided that the shut down would present an opportunity to examine the interior of the generator in order to evaluate the effectiveness of the nickel plating. Upon disassembling the 4-cell unit, some corrosion was observed on the plates. This was explained by the fact that the plates had been vapor blasted with a mixture of water and alumina after they were nickel plated. This cleaning process had abraded away machining burrs, thus exposing bare magnesium to the KOH electrolyte. As a result of this information, careful deburring of the bi-polar plates for the 26-cell unit was accomplished prior to the plating operation. In addition it was decided that a thin, 0.02 mil, coat of gold should be put on top of the nickel plate to afford further corrosion protection. The 4-cell generator was then reassembled and the test continued. The test was finally stopped after a total time of 365 hours in order that adjustments could be made in the test rig in preparation for testing the 26-cell unit.

During operation of the 4-cell unit its performance was checked as a function of inlet air flowrate and inlet air pressure. As indicated from the data presented in Figure 19(a) the performance was almost identical at air flow rates of 3 and 5 times theoretical, but a decided increase in voltage was needed at a flow rate of 2 times theoretical. After 225 hours of total operation, a 6.3 hour experimental run was made with an inlet air pressure of 8 psia. From the results presented in Figure 19(b) the performance curve taken at 8.0 psia, after 3 hours operation at this pressure, is very similar to the generator performance observed after the air inlet pressure was returned to atmospheric pressure.



(a) Effect of Flowrate



(b) Effect of Pressure

FIGURE 19 FOUR-CELL GENERATOR PERFORMANCE

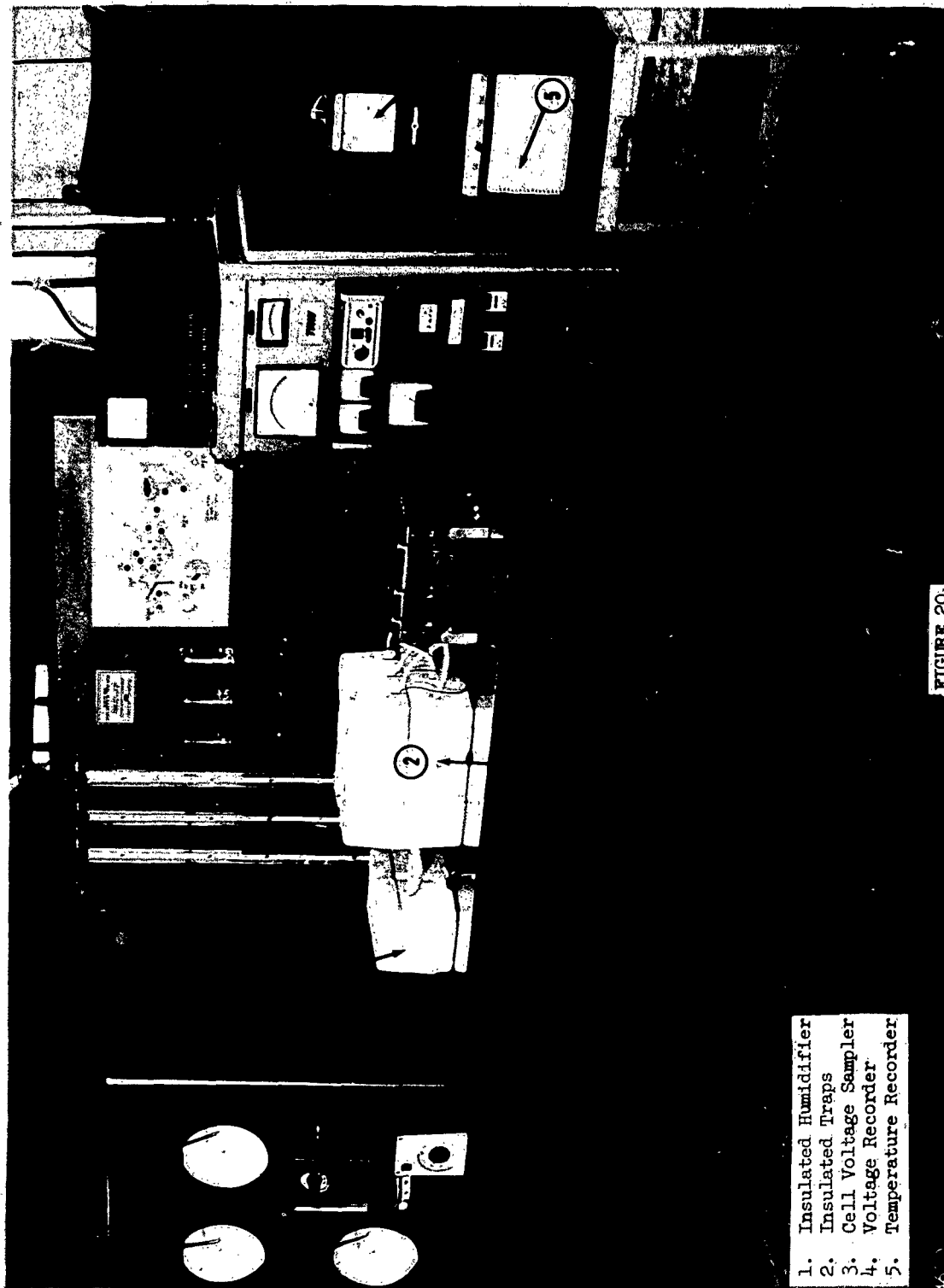
Twenty-Six Cell Generator

Testing of the 0.2 lb/hr system was that necessary to verify that all oxygen production rate regulating equipment, including the thermal and humidity controls, were operating properly. Measurements were made that showed no contaminants were present in the oxygen output. Cell performance sensitivity to ambient pressure and to pressure differentials across the electrolyte filled matrix were studied. The system was then operated over a period of weeks which verified its conformance to the design objectives.

During the time that the 26-cell model was operated at TRW a semi-continuous record was made of gas temperatures at various locations in the test rig and of the concentrator temperature itself. The total voltage and the voltage of the 26 individual cells were also recorded. This data provides a permanent record of generator performance and conditions. Shown in Figure 20 is a photograph of the 26-cell laboratory model in operation. Also shown in the photograph are the multipoint recorder and the dual channel voltage recorder used to record the data taken on the program. One channel of the voltage recorder continuously monitored the terminal or total voltage. The second channel recorded individual cell voltages from a signal provided by the cell voltage sampler.

During operation of the generator at TRW it was demonstrated that the effect of variations in operating parameters depended upon the "condition" of the generator. If the unit was operated for a period of time in an out-of-balance moisture condition the performance was more sensitive to flowrate, air inlet pressures, effects of temperature, etc. An out-of-balance condition refers to operation where the water vapor pressure of the inlet air doesn't match the electrolyte vapor pressure at the generator operating temperature. Even when the unit was in moisture balance, the effects of variations in an operating parameter was not always consistent. This is not unexpected when one considers that the observed response of the generator changes in the operating conditions is actually the sum of changes in 26 separate cells. Each of the 26 cells has, within limits, its own response to a change in operating conditions. This results because individual electrodes vary slightly in activity. Also each cell has a slightly different environment resulting from its position in the series stack, may see slightly different air flows due to small variations that occur during fabrication of the ducts, etc.

Although every attempt was made to duplicate the individual cells, it was impossible to ensure that all electrodes were exactly identical or that the cells at each end of the stack would experience the same thermal environment as the cells located in the middle. When the flowrate was decreased to less than three times the theoretical flowrate, for example, the voltage across the concentrator increased. Not all 26 cells in the generator, however, required the same increase in voltage. Such variations, therefore, lead to a different generator "condition" depending upon the prior operating history and the manner in which the parameter was varied. The more rapid the variation, for example, the less chance the cells have to reach a steady state condition. In the sections to follow the general effects are described. The effects, however, require a backlog of operating data to enable strict interpretation. Interpretation of the change in the 26-cell generator voltage as a function of change in operating parameters on an absolute basis is extremely complex.



1. Insulated Humidifier
2. Insulated Traps
3. Cell Voltage Sampler
4. Voltage Recorder
5. Temperature Recorder

FIGURE 20.
LABORATORY MODEL IN OPERATION

Demonstrated Operating Life

Three-hundred forty five hours were accumulated on the 26-cell model and control system while operated at TRW. Four of these 26-cells were operated for over 700 hours. During the course of the experimental program the performance of the generator went through several cycles where it appeared as if the performance was degrading. In all cases it was shown that the gradual increase in voltage required could be attributed to an imbalance in the cell moisture since the unit recovered when balance was restored. At the time of shut down the generator was delivering 11.7 amps ($0.2 \text{ lb O}_2/\text{hr}$) at 25 volts.

Effect of Flowrate

The performance of the 26-cell model, as was the case with the 4-cell unit, is relatively independent of flowrates over 3 times the theoretical. Below this level a decided dependency exists. The effect of the flowrate was less significant at low current densities. As the current level increased the effect of flowrate increased. The data presented in Figure 21 illustrates the effect of flowrate on generator performance.

Effect of Inlet Pressures

At various times the generator was operated with low inlet pressures, with the outlet pressures being less than 1 psia lower than the inlet. At an inlet air pressure of 10.6 psia the generator voltage for the 11.7 amp load varied with mass flowrate as shown in Figure 22.

Following operation at 10.6 psia the inlet pressure was further decreased to 6.5 psia. At the same current, 11.7 amps, and an air flowrate of 3 times the theoretical the observed voltage was 26.1 volts, which after 1.2 hours had decreased to 24.8 volts. After returning to atmospheric conditions the observed voltage, while maintaining a 3 times theoretical flow and a current of 11.7 amps, was 23 volts. With time, this increased to 25 volts. The reason for the improved performance of the unit immediately after operation at less than atmospheric pressure is found by examining the individual cell voltage data. During operation at less than atmospheric pressure, several cells that initially had higher than average voltages "recovered" or decreased in voltage. This would indicate that their higher voltage levels resulted from an effect associated with operation at less than atmospheric pressure.

Effect of Operating Temperature

Extensive testing was not made on the effects of temperature on performance. The prime objective was delivery of a working laboratory model and a degree of caution was observed in attempting to experiment outside the realms of the design. As an indication of the effect of temperature, however, one can cite the improvement noted in performance when the temperature was increased. Typical would be the 1.0 volt or so decrease in voltage when the generator goes from room temperature to operating temperature. It should also be noted that the downward trend in voltage due to temperature rise on start-up is counter balanced by a natural increase in voltage due to the time dependent polarization phenomena.

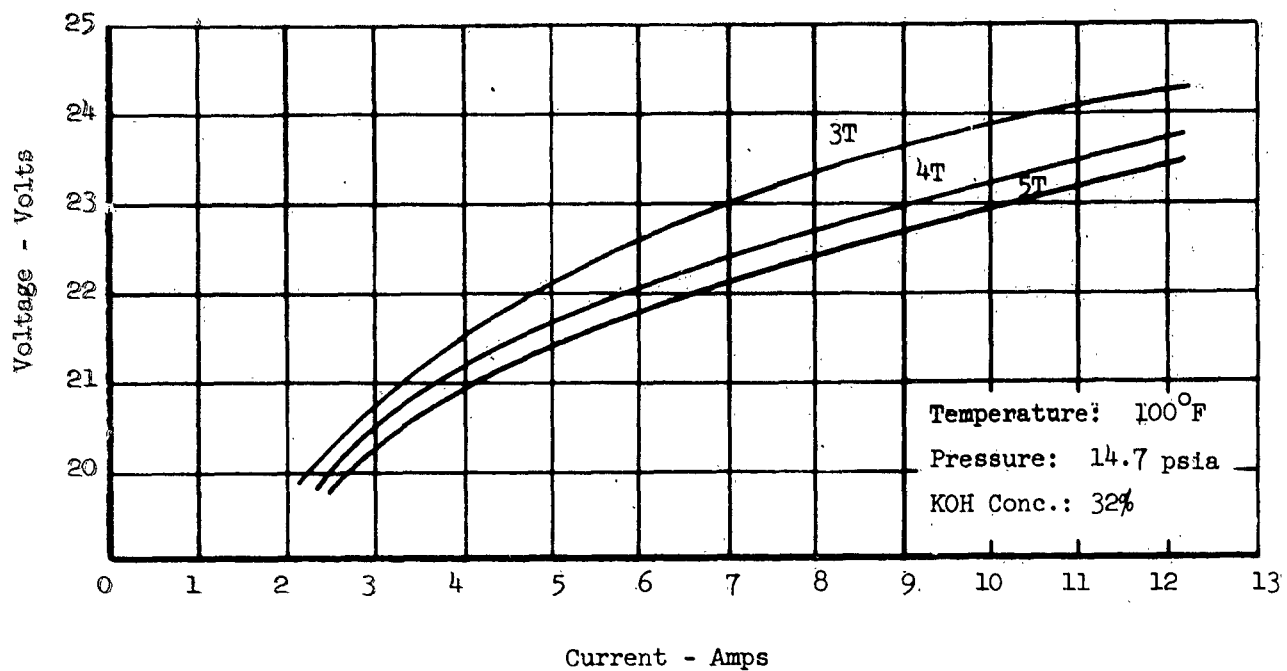


FIGURE 21
EFFECT OF FLOWRATE

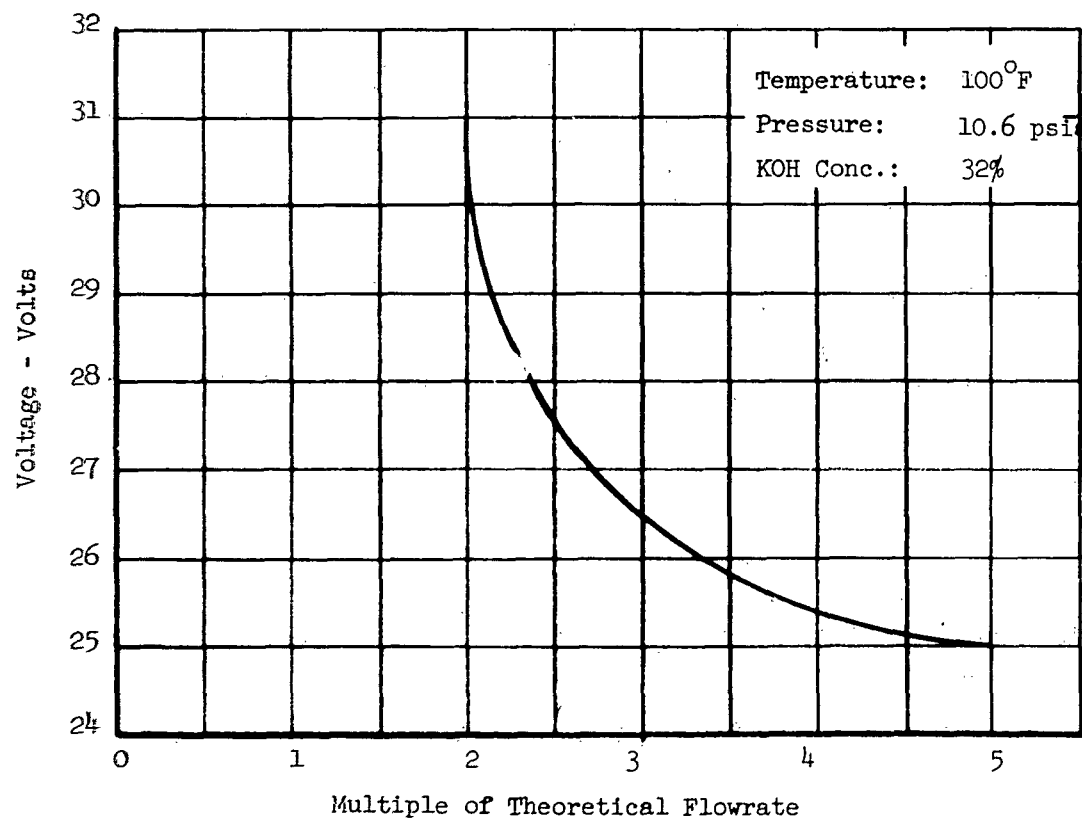


FIGURE 22
EFFECT OF FLOWRATE AT REDUCED PRESSURE

As a further example of the effect of temperature, a case in which the generator was operated with the cooling air inadvertently left off can be cited. Upon restarting the generator after a shutdown at 320 hours, it reached an improved performance of 15.0 amps and 19 volts before it was realized that the cooling air was not on. The generator temperature was found to be 125°F . After cooling the generator back to 95°F the voltage had increased to 23.5 volts with the same 15.0 amp input. At 125°F the average voltage per cell was 0.73 compared to the 0.92 volts at 95°F . Since the laboratory generator and associated equipment were not designed for operation at more elevated temperatures, operation was continued at the lower temperature. Although no limitations are envisioned to generator operation at higher temperatures, the need to deliver a working model cautioned against testing at more such conditions in spite of the attractive performance that may have resulted.

Oxygen Output

Several times during the test program the generator was operated at current levels far in excess of the design point. In Figure 23 are plotted such performances for the 4- and 26-cell units. The maximum oxygen output was about 0.6 lb/hr for the 26-cell unit and about 0.1 lb/hr for the 4-cell unit.

Oxygen Purity

Since the gas generating principle is electrochemical in nature and hydroxyl ions are the only anions in the matrix, oxygen is the only gas that can be evolved from the anode electrodes. This reaction is the basis of the commercial preparation of oxygen using an electrolysis cell.

Three separate techniques were used to evaluate the purity of the oxygen: (1) coulometric balances which relate the current passed per unit time with the volume of oxygen generated; (2) use of a direct reading Beckman Model D-2 oxygen analyzer; and (3) a conventional gas chromatograph. In all cases the purity of the oxygen was found to be between 99.5 and 100 per cent after the sample was corrected for the water vapor contained in it.

The coulometric method is based upon Faraday's Laws of Electrolysis and is an accepted standard for determining the purity of gases generated electrochemically. With this technique the oxygen generated is collected for a known period of time at a constant current level. The volume of gas collected equals, to within 0.3 per cent the volume of oxygen calculated from the measured coulombs (amp-seconds).

Periodically during the testing the oxygen was analyzed with a Beckman D-2 oxygen analyzer calibrated each time with dry atmospheric air. The purity level was always found to be one hundred per cent.

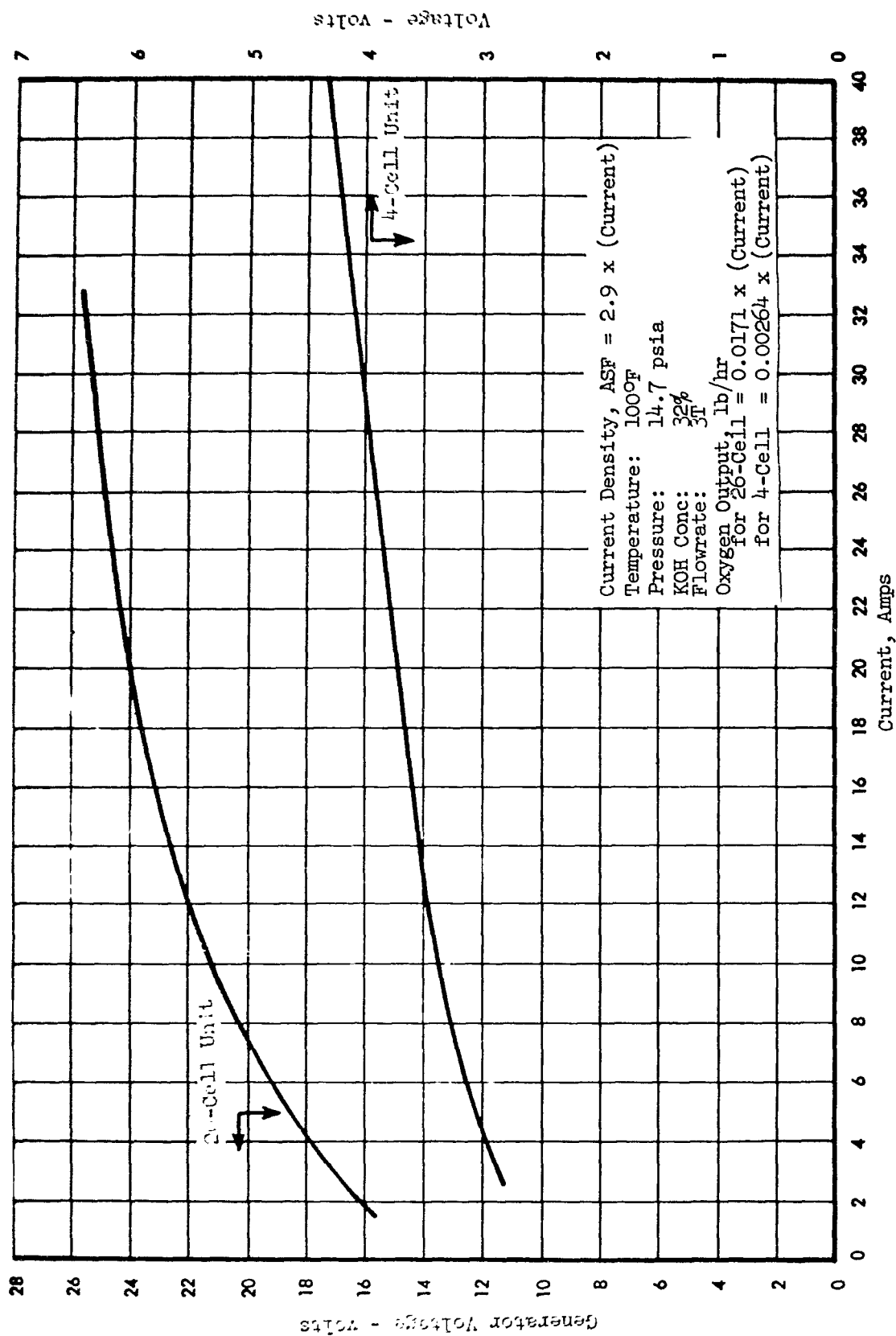
Several oxygen samples were taken for gas chromatographic analysis. The oxygen purity was generally found to be higher than commercial oxygen having a purity minimum of 99.6%. One such analyses showed that the oxygen contained 4.7% nitrogen. Upon rechecking the stability of the oxygen generator to pressure differentials it was observed that a leak had developed between the oxygen and air compartments. Reloading the generator with electrolyte eliminated the leak. No other contaminants were ever found in the gas. The presence of any nitrogen in the oxygen output stream would indicate that some of the air has direct access to the oxygen.

Stability to Pressure Differentials

An important feature of the design is that the electrolyte filled matrix prevents mixing of the gases in the separate compartments. Pressure tests on single cells show they could withstand differentials between gas compartments of greater than 10 psig. Initially the 2- and 4-cell units withstood 6 psi differentials, but with time the upper limit decreased to 3 psi due to (1) a relaxing of the bolts following initial operation and (2) evaporation of water from the electrolyte which decreases its volume and decreases pressure differential stability.

The pressure differential that could be tolerated between the inside and outside of the 26 cell unit exceeded 15 psi, although the interior pressure differentials between gas compartments never exceeded 3 psi. Later this value decreased to under 1 psi due to the same causes as in the smaller units. The lower pressure differentials for the 2, 4, and 26-cell units resulted, in part, from the use of the 15 mil gasket instead of the 10 mil that the design called for. This meant that the porous matrix was not compressed to its design thickness. The observed pressure differentials were still above those required by the design criteria.

FIGURE 23
GENERATOR EXTENDED
PERFORMANCE



SECTION V. DESIGN ANALYSIS AND RECOMMENDATIONS

During the time that the concentrating system was being fabricated and tested, consideration was given to various modifications in the design to further optimize and simplify its construction and operation. Some were incorporated into the program and others are recommended for the future.

Design Criteria Evaluation

The design of the deliverable laboratory model of the oxygen concentrator was guided by several design criteria. During the program the generator was demonstrated to be capable of meeting most of these guideline objectives. Conformance to the remaining criteria could only be demonstrated analytically.

A. The multicell system was shown to be capable of operation at full capacity using a 26 volt DC constant current supply. An analysis of power conditioning required to convert a 28 volt DC aircraft power source into a constant current indicated that 2 volts would be required leaving 26 volts to power the concentrator. As a result of the laws of electrochemistry, operation of the concentrator with a constant current of 11.7 amps will provide a continuous oxygen output of 0.2 lb/hr.

B. The concentrator output was pure oxygen, at $70^{\circ} - 5$ F. with a purity greater than 99.5%, after water vapor removal. No contaminants such as carbon monoxide, carbon dioxide, hydrogen, nitrogen or hydrocarbons were found. Electrochemically such contaminants cannot be formed in the oxygen compartments of the concentrator. In the event that the pressure differential between the air and the oxygen compartment exceeds the limit of the operating concentrator it is possible to force air into the oxygen compartment or vice versa. Such, however, is outside the normal mode of operation.

C. The system was able to furnish the oxygen at 0.2 psia (0.4 in Hg) above inlet pressures ranging from 6.5 to 15.5 psia. By increasing compression of the electrolyte matrix, it should be possible to tolerate a 6 psi pressure differential.

D. A control system was designed and incorporated as part of the delivered multicell concentrator. The control system was able to maintain a steady oxygen output rate at any selected production rate from zero to over the full capacity of 0.2 lb/hr. The system controlled the current, the air flow, the operating temperature, and the humidity balance.

E. The unit was demonstrated to be able to attain full capacity operation within seconds subsequent to nonoperation for periods up to 12 days. The generator reached operating temperature within 3 minutes after start-up, but the humidifier design was such that about a half-hour was required to raise it to operating temperature.

F. The multicell concentrator was capable of continuous and intermittent operation with the only maintenance required being the periodic changing of a filter and CO_2 absorber on the inlet air line and the addition of a little water.

G. The 26-cell array was operated in only a horizontal position. The 2- and 4-cell units, however, were operated in a vertical orientation. It can be inferred from these results and from the fact that no free flowing or bulk liquid exists in the concentrator that the unit is capable of operating in any orientation.

H. The concentrator was shown to withstand more than a 20 psi pressure differential between the inside and outside of the unit. It can be concluded, again noting that all the liquid is retained in a porous matrix, that leakage does not occur as a result of orientation.

I. The delivered 26-cell array would weigh 28 pounds if and when the heavy end-plates would be replaced with end-plates providing the same support but with a more open or porous structure. The weight of an optimized model would be less than 15 pounds.

J. All equipment and/or surfaces which contacted electrolyte and high humidity gases were coated or constructed of noncorroding materials.

K. The multicell array was not subjected to any "g" loadings. However, because the electrolyte is held in a porous matrix and the bi-polar plates have the strength and rigidity to retain the cell components from structural damage, the unit should be capable of operating under extensive "g" loading.

Design Improvements

During the program several features were incorporated into the design that were not part of existing technology. These included (a) increasing the electrode area from 36 sq. in. to 50 sq. in., (b) fabrication of 4 and 26-cell arrays and the technology associated with manifolding such multiple cell assemblies, (c) use of a special magnesium alloy having a high thermal conductivity per unit weight that decreased the bi-polar plate weight, (d) use of an O-ring seal instead of a flat gasket (this eliminated the leakage problems associated with flat gaskets), (e) decreasing the sealing edge border around the electrodes and matrix from a width of 0.25 in. to 0.062 in. and 0.2 in., respectively, (this increased the effective electrode area and demonstrated where additional weight can be eliminated from future designs), (f) use of hollow Teflon baffles instead of wire baffles (this decreases weight and eliminates the corrosion potential associated with wire baffles), (g) incorporation of interchangeable oxygen and air compartments that allow experimental evaluation of air electrode performance with two types of manifolding systems, (h) an air cooled fin as the method used for heat removal, (i) a new humidifier design which provided information and demonstrated an air moisturizing technique that is applicable to a flight model concentrator, and, finally, (j) the accumulation of over 700 hours of test time on four of the 26 cells.

Fabrication of the bi-polar plates from magnesium instead of copper, cut machining times one-fourth and minimized weight. The initial concentrator design called for the use of 140 mil magnesium stock to be used for bi-polar plate fabrication, but only 133 mil stock was available. Use of this thickness resulted in a concentrator weight of 3 - 4 pounds more than if the thinner material had been used. Machining the 133 mil stock down to the thinner dimension was not practical at the time.

Problems and Solutions

An attempt to frame the bi-polar plate with a 10 mil coat of alkaline resistant epoxy was found to be more difficult than initially assumed. In experimenting with this technique it was found that the difficulty was not with bonding the epoxy to the bi-polar plate but controlling the thickness to 10 mils. The solution to this problem would have required that a special jig be designed to move and heat the plate while the epoxy was sprayed on. A 10 mil rubber gasket could not be obtained in time for program scheduling and a 15 mil substitute was used.

During the course of the experimental program, cell number 7 of the 26 cells was found to very often require a voltage that was about 1.5 to 2.0 times that of other 25 cells. The reason for this was attributed to partial blockage of one or more of the air compartment gas ducts. It would be suggested that future designs use one larger duct instead of two small ducts per port. A larger duct would be less likely to become plugged with solid particles inadvertently appearing in the concentrator.

The capacity of the test rig was designed for the 0.2 lb/hr. concentrator. At the time the test rig was designed it was not realized that the concentrator might be operated up to 3 times that of the design point. The power supply included with the test rig was limited to only 15 amps. Higher currents, therefore, required paralleling a second power supply with the one provided with the test rig. The cooling capacity of the concentrator was designed for a 364 watt load. During operation of the concentrator at capacities in the range of 0.5 lb/hr, the heat load increases above this level and sustained operation under these conditions is not advisable. The control system suffered from a lag in response time of the equipment. The reliability associated with pneumatic controls, however, warranted its selection in spite of this. The humidifier response was increased by wrapping a heating tape around the outside. A better design would be one in which the heat source is in more intimate contact with the surface on which evaporation occurs.

Design Recommendation

Presented in Table 2 are the results of a design analysis related to further optimizing the concentrator. Compared in this table are the component and total weights for (1) the present model using 183 mil magnesium (2) the model actually designed initially and which required 140 mil magnesium stock, and (3) a projected concentrator of the same basic design, but optimized and using 75 mil magnesium for the bi-polar plates. In calculating the generator weights it was assumed that a more optimized form of end-plate would be used. The total weight for the three models are 28, 22, and 13 pounds, respectively.

Table 2
Component and Total Weight

<u>Component</u>	<u>183 mil stock (1)</u>		<u>140 mil stock (2)</u>		<u>75 mil stock (3)</u>	
	<u>wt., lb</u>	<u>%</u>	<u>wt., lb</u>	<u>%</u>	<u>wt., lb</u>	<u>%</u>
Bi-polar plates (Ni plated Mg)	18.77	67.5	13.09	59.8	7.07	53.4
Electrolyte (35% KOH)	2.91	10.5	2.91	13.3	1.37	10.3
End plates (Ni plated Mg) (6)	2.60	9.4	2.60	11.9	2.60	19.6
Matrix (asbestos)	1.55	5.6	1.55	7.1	0.67	5.1
Electrodes	0.76	2.7	0.76	3.4	0.76	5.7
O-rings (ethylene-propylene)	0.35	1.2	0.35	1.6	0.24	1.8
Insulation (epoxy) (4)	0.54	1.9	0.33	1.5	0.20	1.5
Nuts and Bolts	0.25	0.9	0.25	1.1	0.25	1.9
Insulation (Neoprene) (5)	0.07	0.3	0.07	0.3	0.07	0.7
	<u>27.80</u>	<u>—</u>	<u>21.91</u>	<u>—</u>	<u>13.23</u>	<u>—</u>
	100.0		100.0		100.0	

- 1) Generator weight based on the 183 mil Mg stock used in this program
- 2) Generator designed based on 140 mil Mg stock called for by the design
- 3) Optimized generator based on same configuration and design as that developed by this program
- 4) Between individual bi-polar plates
- 5) Between end-plates and adjacent bi-polar plates
- 6) Optimized end-plate design

The optimized concentrator design includes such changes as (1) decreasing matrix thickness, (2) increasing the effective electrode area by cutting the width of the edge seal around the electrode in half, (3) decreasing the height of the gas compartments, and (4) obtaining an O-ring to match the needed dimension rather than design the bi-polar plate area to match the available O-ring size. A further comparison of these changes between the present model and the optimized model is given in Table 3. The analysis was made assuming that the optimized model would have the same general configuration and method of heat removal. This emphasizes the extent to which the initial model can be improved without including more elaborate design modifications which would make direct comparison difficult.

Performance improvement can be obtained by operation at elevated temperatures to increase electrode efficiencies, i.e., decrease cell voltage. This will decrease the power requirements. Also, combining the humidification and heat removal functions within the concentrator itself would provide for a self-regulating design. Such a design would use evaporative cooling to remove the heat generated and the evaporated water vapor to humidify the air feed. This would eliminate the more extensive controls used with the laboratory model.

Table 3
 Comparison of Generator to be Delivered
 With An Optimized Generator
 Of Same Design

<u>Component</u>	<u>183 Mil Mg Stock</u>	<u>75 Mil Mg Stock</u>
Asbestos		
area dimensions, in	5.0 x 12.5	4.75 x 12.25
thickness, in	0.030	0.015
Electrodes		
area dimensions, in	4.5 x 12.0	4.5 x 12.0
effective area, in	4.25 x 11.75	4.4 x 11.9
thickness, in	0.005	0.005
Bi-polar Plates		
area dimensions, in (a)	15.0 x 6.5	13.5 x 5.4
pin height, in		
air compartment	0.065	0.030
O_2 compartment	0.063	0.015
thickness, including pins, in	0.183	0.075
neoprene gasket thickness, in	0.015	0.025
26-cell Generator		
dimensions, in (a)	15.0 x 6.5 x 6.4	13.5 x 5.4 x 3.6
volume, ft ³ (a)	0.36	0.15
weight, lb	28	13

^(a) Does not include the 12.0 x 0.5 inch cooling fin extending out along two long sides of the generator.

VI. SUMMARY

An electrochemical oxygen concentrator for separating pure oxygen from air has been designed, fabricated, and tested. The concentrator consisted of 26 cells. Each cell was composed of two porous electrodes separated by an electrolyte solution held in a porous matrix. Individual cells were separated with bi-polar plates.

During the experimental program the effects of air flowrates, air inlet pressures, and temperature were measured. A total of 340 hours were accumulated on the 26-cell model with an additional 365 hours of testing time completed on 4 of the 26 cells prior to their being tested as part of the 3.2 lb hr capacity unit.

Considerable reduction in concentrator weight, volume, and power required was projected for more optimized designs. Control simplification was also a part of the design recommendation.

VII. REFERENCES

1. Edmund C. Potter, "Electrochemistry-Principles and Applications", Cleaver-Hume Press Ltd., 1956, p. 124.
2. ibid, p. 141
3. E. R. G. Eckert and R. M. Drake, Jr., Heat and Mass Transfer, McGraw-Hill Book Company, New York, 1959.
4. H. Schlichting, Boundary Layer Theory, McGraw-Hill Book Company, New York, 1960.
5. D. R. Richards, "How to Design Fluid Flow Distributors", Chemical Engineering, May 1, 1961.
6. W. L. McCabe and J. C. Smith, "Unit Operations of Chemical Engineering", McGraw-Hill Book Company, New York, Pg 75-79, 1956.

AFFIX: DESIGN CALCULATIONS

The purpose of these appendices is to facilitate the understanding and testing of the oxygen generator. It includes:

- (1) A description of the thermal analyses used to estimate generator temperatures and generator cooling air requirements.
- (2) A description of the calculations made in designing the gas manifolds and ducts as required in the generator and humidifier.

Symbols

A	Active electrode area
C_o	Orifice coefficient
c_p	Specific heat of air at constant pressure
d_h	Hydraulic diameter of air passage between fins
E	Voltage applied across each cell
F	Generator air supply flowrate
f_c	Dimensional consistency factor
h	Convective heat transfer coefficient
I	Current flowing through each cell
K_c	Contraction factor
K_e	Expansion factor
k	Thermal conductivity
L	Length between duct passages
ℓ	Equivalent length
m	Flow factor
n	Number
Nu	Nusselt number
P	Pressure
ΔP	Pressure drop
P_d	Hydraulic power
Pr	Prandtl number
q	Heat flux per cell
Q	Thermal energy flux per unit volume
Re	Peynolis number

Symbols

T	Theoretical multiple
Δt	Temperature difference
V	Bulk velocity of air; linear velocity of air
w	Mass flow rate of air per cooling passage; oxygen output from generator
x	Width, dimension perpendicular to long edge of cell
y	Length, dimension parallel to long edge of cell
z	Thickness, dimension perpendicular to plane of cell
ϵ	Equivalent height of surface roughness
λ	Friction factor
μ	Absolute viscosity of air
ρ	Density of air

Subscripts

a	Air
b	Bi-polar plate body in active region
c	Active cell
d	Air passage or duct between two adjacent fins
D	Hydraulic diameter
e	Electrode
f	Bi-polar plate fin
F	Field
g	Bi-polar plate body in gasket region
m	Electrolyte-filled matrix
p	Bi-polar plate pin
s	Electrode-matrix-electrode sandwich
x	In x direction
y	In y direction
1,2,3,- 5,6,7	Opposite sides of bi-polar plate; individual pressure drops

Superscripts

- Average along length

A) THERMAL ANALYSIS OF OXYGEN GENERATOR

Analytical Methods and Assumptions

Local temperatures and coolant requirements for the oxygen generator have been determined by using standard heat transfer and fluid mechanics' analyses.

The oxygen generator consists of a stack of rectangular cells, cooled by air flowing between fins which project from the longer two sides of the stack. Each cell consists of two electrodes with an electrolyte-filled porous matrix between them. Good electrical and thermal contact are obtained by clamping the electrode-matrix-electrode "sandwich" between two metal plates. Air and oxygen flow passages are machined into these plates so that most of the electrode area is exposed to the gas passages; the plates then contact the electrodes in a lattice of small square areas or "pins". The metal plates are bi-polar; that is, each plate contacts two electrodes; the cathode of one cell and the anode of the adjacent cell. The top and bottom plates of the stack each contact only one electrode, and function as electrical input terminals to the stack. Throughout the stack, adjacent bi-polar plates are electrically isolated from each other by a 0.015 inch thick rubber gasket insulator; edge sealing is accomplished by O-ring gaskets. The bi-polar plates extend outside of the gasket area on the two long sides as thin fins; it is these fins which are cooled by forced convection of air in order to reject the waste heat of the cell.

The chief heat transfer path in the generator is as follows: Electrical energy is dissipated in the electrodes and in the electrolyte-filled matrices between them. The resulting thermal energy is transferred by conduction along the electrodes and matrices to the bi-polar plate contact areas, through the pins to the main bodies of the bi-polar plates, and along the plates past the gaskets and into the projecting fins. Heat is then rejected to the cooling air in a forced convection process. Two other possible modes of heat rejection are expected to be unimportant: (1) Conduction through the other four faces of the cell stack and rejection by natural convection to the ambient air; and (2) convection due to the air and oxygen flowing through the cell.

For the analysis, the heat transfer process has been assumed to be steady and essentially one-dimensional with the ends, top, and bottom of the stack assumed to be perfectly insulated. The thermal conduction in each cell is assumed to be in a direction perpendicular to the cooling air velocity vector; that is, conduction occurs mainly in the X direction. The effects of the gases flowing within the cells will be neglected throughout the analysis.

Electrical Dissipation

In the analysis to follow it is assumed that a maximum heat load will have to be removed. Under this assumption the heat load becomes

$$\left(\begin{array}{l} 304 \text{ amps} \\ 0.2 \text{ lb } O_2/\text{hr} \end{array} \right) \quad \left(\begin{array}{l} 1.2 \text{ volts/cell} \end{array} \right) \quad \text{or 365 watts.}$$

The minimum heat load anticipated would be for operation with each cell requiring 0.8 volts or a total of 243 watts for all cells. The average load, such as is expected during operation of the generator with an air inlet pressure of 6.5 psia, would be 304 watts, i.e. each cell requiring 1.0 volts.

Heat Transfer in Electrodes and Matrix

Assuming that the electrical dissipation is steady in time and is distributed uniformly over the active area of each cell, a two-dimensional thermal conduction problem in the electrode-matrix-electrode sandwich can be formulated and solved analytically. The solution will be a Fourier series of the products of trigonometric and hyperbolic functions and will be relatively difficult to evaluate. An alternate approach is to set up an equivalent one-dimensional problem, selected so as to set an upper bound on the temperature variation in the sandwich, and so give a conservative answer. This approach has been followed.

The active electrode area on either side of a cell is the cell area minus the total pin contact area,

$$A = x_{cyc} - \pi p x_p y_p .$$

The thermal energy generated per unit volume of active sandwich is then

$$\mathcal{Q}_s = \frac{Q}{A (2z_e + z_m)}$$

The maximum temperature difference in the sandwich is then

$$\Delta t_s = \frac{\mathcal{Q}_s}{2k_s} \ell_s^2,$$

where ℓ_s is an equivalent one-dimensional conduction path length and k_s is the effective thermal conductivity of the sandwich (see Reference 3). A conservative temperature difference will be calculated if ℓ_s is chosen as half the distance between the centerlines of diagonally adjacent pins:

$$\ell_s = \frac{1}{2} \sqrt{\left(\frac{x_c}{\pi p_x}\right)^2 + \left(\frac{y_c}{\pi p_y}\right)^2} .$$

For a square pin

$$\ell_s = \frac{x_c}{\pi p_x} \cdot \sqrt{\frac{2}{2}} = \frac{y_c}{\pi p_y} \sqrt{\frac{2}{2}} .$$

Assuming that the sandwich is thin compared to this length, the effective conductivity is

$$k_s = \frac{2 k_e z_e + k_m z_m}{2 z_e + z_m} .$$

Heat Transfer in Bi-Polar Plate Pins

Although the bi-polar plate pins which contact the electrodes are roughly cubical, a first approximation to the temperature difference across them can be obtained by assuming a one-dimensional thermal conduction process. If the calculated temperature difference is significant, a more exact analysis will be necessary. Assuming that the temperature difference across the air-side pins is the same as that across the oxygen-side pins; that is, that there is no temperature variation across the electrode-matrix sandwich in the z-direction or across the main body of the bi-polar plate in the z-direction;

$$\Delta t_p = \frac{Q}{k_b \eta_p x_p y_p} \cdot \frac{z_{pl} z_{p2}}{z_{pl} + z_{p2}} .$$

Since the pins must be in good electrical contact with the electrodes, it may be assumed that the thermal resistance of the junctions is negligible, so that the electrode and the adjacent pin face are at the same temperature.

Heat Transfer in Bi-Polar Plate Body

Assuming that the pins are spaced close enough so that the heat flux into the body of the bi-polar plate can be considered uniformly distributed over the cell area,

$$\mathcal{Q}_b = \frac{Q}{x_c y_c z_b} .$$

The temperature difference in the plate body between the center of the cell and the edge of the active area is

$$\Delta t_b = \frac{\mathcal{Q}_b}{2k_b} \left(\frac{x_c}{z} \right)^2 .$$

In the sealing region the bi-polar plate is relatively thick, but has bolt holes and recesses for the electrode-matrix sandwich and the O-ring machined into it. A conservative approximation to the temperature difference across this region can be obtained by assuming that the plate has a uniform thickness, z_g , equal to its minimum actual thickness in the sealing region, and using the one-dimensional conduction equation. For each side of the cell,

$$\Delta t_g = \frac{Q x_g}{2k_b y_g z_g} .$$

Forced Convection Heat Transfer

If a cooling air temperature rise across the generator is specified, the air flowrate for each passage formed by two adjacent fins and an external shroud is

$$w = \frac{Q}{2 c_p \Delta t_a} .$$

The bulk velocity of the air is then

$$V = \frac{v}{\rho x_f z_d} .$$

The hydraulic diameter of the fin passage is

$$D = \frac{4 x_f z_d}{2(x_f + z_d)} ,$$

and the Reynolds number based on this diameter is

$$Re_D = \frac{\rho V D}{\mu} .$$

For a constant viscosity fluid in hydraulically fully-developed flow at diameter Reynolds numbers above 2300, Reference 3 gives a semi-empirical heat transfer correlation:

$$\overline{Nu}_D = 0.116 \left[\left(Re_D \right)^{2/3} - 125 \right] \left[Pr \right]^{1/3} \left[1 + \left(\frac{D}{y_f} \right)^{2/3} \right] ,$$

where the average diameter Nusselt number is defined as

$$\overline{Nu}_{D,} = \frac{\bar{h} D}{k_a} .$$

In order to insure that the flow is fully-developed and turbulent through the entire fin passage, an orifice assembly should be placed across the passage entrance. The above correlation predicts an infinite heat transfer coefficient at the passage entrance, but this will not be strongly reflected inside the cell because of thermal conduction in the y direction which has been ignored for this analysis.

Heat Transfer in Fins

The difference between the temperature at the base of the fins (outside edge of gasket region) and the bulk temperature of the cooling air can now be evaluated. For a thin rectangular fin with no heat rejected from the outside edge,

$$\Delta t_f = \frac{Q}{2\pi k_b y_f z_f \tanh mx_f} ,$$

where m is a fin factor defined as

$$m = \sqrt{\frac{2h}{k_b z_f}} ,$$

see Reference 3

Cooling Air Pressure Drop

For hydraulically fully-developed flow in the fin passage, the pressure drop will be

$$\Delta P_d = \lambda_d \frac{y_f}{D} \left(\frac{1}{2} \rho v^2 \right) .$$

where the friction factor for the passage, λ_d , is a function of the diameter Reynolds number, Re_D , and of the relative roughness of the fin passage walls, ϵ/D . This function is presented in graphical form in Reference 4.

Cooling Air Pumping Power

The hydraulic power necessary to force the air through the inlet fin passages is

$$P = \frac{2 \eta_c w (\Delta P_i + \Delta P_d)}{\rho} .$$

The electrical power required for a motor-powered blower will be this hydraulic power divided by the product of the blower efficiency and the motor efficiency.

B) SAMPLE HEAT TRANSFER CALCULATIONS

In order to further explain the analysis, and to illustrate the use of units and conversion factors, a complete sample calculation of the thermal analysis for the generator follows. Calculations will be performed in the same order as presented in the preceding section.

Electrical Dissipation In Each Cell

$$E = 1.2 \text{ volts} \quad (\text{maximum cell potential expected to be required for } 11.7 \text{ amps})$$

$$I = 11.7 \text{ amperes} \quad (\text{current required for each of 26 cells to provide } 0.2 \text{ lb of oxygen per hour})$$

$$\begin{aligned} Q &= (1.2) (11.7) = 14.04 \text{ watts} \\ &= (14.04) (3.41) = 48 \text{ Btu/hr} \end{aligned}$$

Heat Transfer in Electrodes and Matrix

Cell dimensions used in these calculations are representative and approximately the cell dimensions in the assembled unit. Some minor modifications of these numbers were made during the actual cell assembly.

$$x_c = 4.25 \text{ inch}$$

$$y_c = 11.75 \text{ inch}$$

$$\eta_p = 1060$$

$$x_p = 0.062 \text{ inch}$$

$$x_c = 0.062 \text{ inch}$$

$$A = (4.25) (11.75) - (1060) (0.062)^2 = 45.8 \text{ in}^2$$

$$z_e = 0.002 \text{ inch}$$

$$z_m = 0.026 \text{ inch}$$

$$\alpha_s = \frac{48}{(45.8)[(2)(0.002) + 0.026]} = 35.1 \frac{\text{Btu}}{\text{hr in}^2}$$

$$\frac{x_c}{\gamma_{px}} = \frac{y_c}{\gamma_{py}} = 0.218 \text{ inch}$$

$$l_s = (0.218)(0.707) = 0.154 \text{ inch}$$

$$k_e = 8 \frac{\text{Btu}}{\text{hr ft F}}$$

$$k_m = 0.36 \frac{\text{Btu}}{\text{hr ft F}}$$

$$k_s = \frac{(2)(8)(0.002) + (0.36)(0.026)}{(2)(0.002) + 0.026} = 1.37 \frac{\text{Btu}}{\text{hr ft F}}$$

$$\Delta t_s = \frac{(35.1)(0.154)^2(12)}{(2)(1.37)} = 3.65 \text{ F}$$

Heat Transfer in Bi-Polar Plate Pins

$$k_b = 77 \frac{\text{Btu}}{\text{hr ft F}} \text{ (for magnesium alloy)}$$

$$z_{p1} = 0.070 \text{ inch}$$

$$z_{p2} = 0.063 \text{ inch}$$

$$\Delta t_p = \frac{(48)(12)}{(77)(1060)(0.062)^2} \cdot \frac{(0.070)(0.063)}{0.070 + 0.063} = 0.061 \text{ F}$$

Heat Transfer in Bi-Polar Plate Body

$$z_b = 0.035 \text{ inch}$$

$$\alpha_b = \frac{48}{(4.25)(11.75)(0.035)} = 27.5 \frac{\text{Btu}}{\text{hr in}^3}$$

$$\Delta t_b = \frac{(27.5)(2.125)^2}{(2)(77)} = 8.08 \text{ F}$$

$$x_g = 1.12 \text{ inch}$$

$$y_g = 11.87 \text{ inch}$$

$$z_g = 0.106 \text{ inch}$$

$$\Delta t_g = \frac{(48)(1.12)(12)}{(2)(77)(11.87)(0.106)} = 3.33 \text{ F}$$

Forced Convection Heat Transfer

$$c_p = 0.24 \frac{\text{Btu}}{\text{lb m F}}$$

$\Delta t_a = 10 \text{ F}$ (This value is specified as a design criteria in calculating the mass flowrate of required cooling air)

$$w = \frac{(48)}{(2)(0.24)(10)} = 10 \frac{\text{lb}_m}{\text{hr}}$$

$$\rho = 0.075 \frac{\text{lb}_m}{\text{ft}^3} \quad \text{at 1 atmosphere pressure and } 70^\circ\text{F}$$

$$x_f = 0.50 \text{ inch}$$

$$z_d = 0.163 \text{ inch}$$

$$v = \frac{(10)(144)}{(0.075)(0.50)(0.163)} = 2.36 (10)^5 \frac{\text{ft}}{\text{hr}}$$

$$= \frac{2.36 (10)^5}{3600} = 65.5 \frac{\text{ft}}{\text{sec}}$$

$$D = \frac{(4)(0.50)(0.163)}{(2)(0.50 + 0.163)} = 0.246 \text{ inch or } 0.0205 \text{ ft}$$

$$\mu = 1.22(10)^{-5} \frac{\text{lb}_m}{\text{ft sec}}$$

$$Re_D = \frac{(0.075)(65.5)(0.0205)}{(1.22)(10)^{-5}} = 8230$$

$$Pr = 0.71$$

$$y_f = 12.00 \text{ inch}$$

$$\overline{Nu}_D = (0.116) \left[\frac{(8230)^{2/3} - 125}{1} \right] (0.71)^{1/3} \left[1 + \left(\frac{0.246}{12.00} \right)^{2/3} \right]$$

$$= 31.4$$

$$k_a = 0.0151 \frac{\text{Btu}}{\text{hr ft F}}$$

$$\bar{h} = \frac{(31.4)(0.0151)}{0.0205} = 23.1 \frac{\text{Btu}}{\text{hr ft}^2 \text{F}}$$

Heat Transfer in Fins

$$z_f = 0.035 \text{ inch}$$

$$m = \sqrt{\frac{(2)(23.1)(12)}{(77)(0.035)}} = 14.37 \text{ ft}^{-1}$$

$$\Delta t_f = \frac{(48)(144)}{(2)(14.37)(77)(12.00)(0.035) \tan h \left[\frac{(14.37)(0.50)}{12} \right]} = 13.87 \text{ F}$$

Cooling Air Pressure Drop

$$\epsilon = 0.001 \text{ inch}$$

$$\frac{\epsilon}{D} = \frac{0.001}{0.246} = 0.00406$$

$$\lambda_d = 0.038$$

$$\Delta p_d = \frac{(0.038)(12.00)(0.075)(65.5)^2}{(0.246)(2)(32.17)} = 9.27 \frac{\text{lb f}}{\text{ft}^2}$$

$$= \frac{9.27}{5.20} = 1.78 \text{ inch H}_2\text{O}$$

Cooling Air Pumping Power

$$\eta_c = 26$$

$$P = \frac{(2)(26)(10)(9.27 + 26.1)}{0.075} = 2.45(10)^5 \frac{\text{lb f ft}}{\text{hr}}$$

$$= \frac{(2.45)(10)^5 (1.356)}{3600} = 92.3 \text{ watts}$$

Summary of Results

If a cooling air inlet temperature of 75 F is assumed, the calculated temperature through a cell may be summarized as follows:

End of Generator at Cooling Air Inlet

Air inlet temperature	75.0 F
Bi-Polar plate temperatures	
Fin base	75.0 + Δt_f = 88.9 F
Edge of active area	88.9 + Δt_g = 92.2 F
Centerline	92.2 + Δt_b = 100.3 F
Pin-electrode contact temperature	100.3 + Δt_p = 100.4 F
Maximum electrode temperature	100.4 + Δt_s = 104.0 F

End of Generator at Cooling Air Exhaust

Air exhaust temperature	85.0 F
Bi-polar plate temperatures	
Fin base	98.9 F
Edge of active area	102.2 F
Centerline	110.3 F
Pin-electrode contact temperature	110.4 F
Maximum electrode temperature	114.0 F

This temperature profile ($^{\circ}$ F) is shown schematically as:

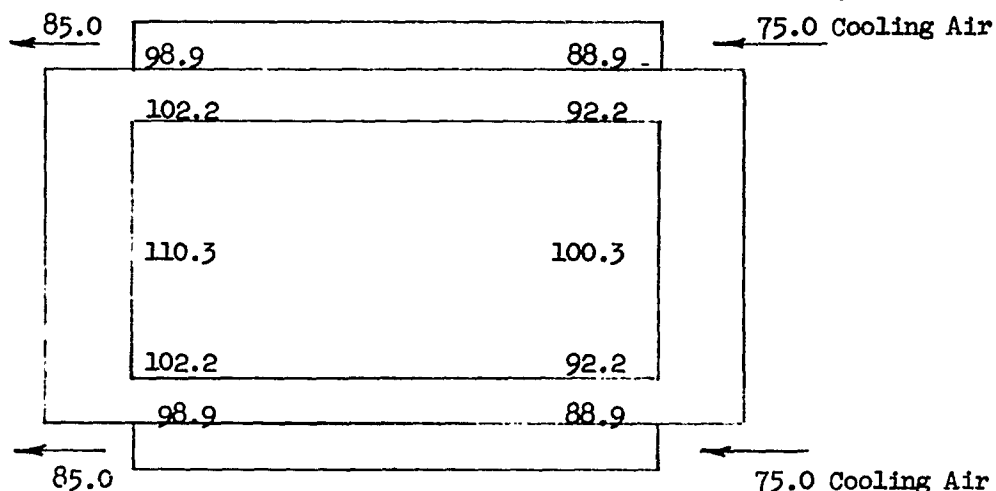


FIGURE B-1
BI-POLAR PLATE TEMPERATURE PROFILE

Generator Gas Port Design

The following calculations illustrate the manner in which the oxygen generator gas manifolds and ducts were designed.

Flow Conditions:

Flowing media: air
Temperature: 104°F, average temperature between the maximum and minimum electrode temperature.
Pressure: 1 atmosphere
Maximum Flowrate: 0.892 SCFM (5 times the theoretical flowrate for generating 0.2 lb per hour of oxygen)

C) AIR FLOWRATE CALCULATION

Two-tenths of a pound of oxygen per hour represents a volume flowrate of 2.24 SCFH. Since air contains approximately 21% oxygen, the theoretical flowrate of air required to deliver 0.2 lb O₂/hr is 2.24/0.21 or 10.7 SCFH. The air flowrate, F, to be supplied to the generator for any current loading, I, and any desired multiple of the theoretical minimum air flow, T, can be calculated from the expressions

$$F = \frac{0.2 \text{ lb O}_2/\text{hr}}{11.7 \text{ amps}} \quad (I) \quad \frac{10.7 \text{ SCFH}}{0.2 \text{ lb O}_2/\text{hr}} \quad (T)$$

or

$$F = 0.912 (I)(T) \text{ in SCFH or } 0.0152 (I)(T) \text{ in SCFM}$$

where I is in amps and T is the dimensionless multiple of the theoretical air flowrate.

Using this calculational procedure as an example, Table C-1 was prepared relating generator current or O₂ output and the theoretical air flows required for producing this oxygen from the 26 module unit.

D) GENERATOR PORT DESIGN

For the generator bi-polar plate (See Figure D-1) the design objective is to specify the diameter of the gas exit and inlet ducts and the pressure drop across the generator.

1) Calculation of Duct Diameter

To avoid unequal air distribution between each of the 26 air compartments of the generator requires that the pressure drop, through the gas ducts feeding the air compartments, be 100 or more times the pressure drop experienced by the air feed.⁽⁵⁾ The air feed pressure drop is that resulting from the flow of the inlet air down the entire length of the port passage as it is formed by stacking together 26 bi-polar plates. The proper duct diameter to meet this requirement was determined as follows:

$$\text{Reynold's number down port passage} = \frac{D V \rho}{\mu}$$

$$D = \frac{7}{16} \text{ in} = 3.65 \times 10^{-2} \text{ ft} \quad = \text{port passage diameter}$$

$$A = 1.05 \times 10^{-3} \text{ ft}^2 \quad = \text{port cross sectional area}$$

$$V = \frac{892!}{2(60 + 1.05 \times 10^{-3})} = 7.10 \text{ ft/sec} = \text{air velocity thru port passage}$$

$$\rho = 7.14 \times 10^{-2} \text{ lb/ft}^3 \quad = \text{air density}$$

$$\mu = 1.25 \times 10^{-5} \text{ lb/ft-sec} \quad = \text{air viscosity}$$

TABLE C-1
THEORETICAL AIR FLOW RATES

O_2 Output, lb/hr	Current, amps	Theoretical Air Flow Rate - SCFM				
		1 Times	2 Times	3 Times	4 Times	5 Times
0.017	1.0	0.0152	0.0304	0.0457	0.0609	0.0761
0.043	2.5	0.0381	0.0762	0.114	0.152	0.191
0.085	5.0	0.0761	0.152	0.228	0.304	0.381
0.128	7.5	0.114	0.228	0.342	0.457	0.571
0.171	10.0	0.152	0.304	0.457	0.609	0.761
0.200	11.7	0.178	0.357	0.535	0.715	0.892
0.214	12.5	0.190	0.381	0.571	0.761	0.952
0.256	15.0	0.228	0.457	0.685	0.913	1.14
0.295	17.5	0.266	0.533	0.799	1.07	1.33
0.342	20.0	0.304	0.609	0.913	1.22	1.52
0.384	22.5	0.342	0.685	1.03	1.37	1.71
0.430	25.0	0.380	0.761	1.14	1.52	1.90
0.470	27.5	0.418	0.837	1.26	1.67	2.09
0.513	30.0	0.457	0.913	1.37	1.83	2.28
0.555	32.5	0.494	0.989	1.48	1.98	2.47
0.598	35.0	0.532	1.07	1.60	2.13	2.67
0.642	37.5	0.571	1.14	1.71	2.28	2.86
0.684	40.0	0.609	1.22	1.83	2.44	3.06

The relationship between oxygen generated, w , in lb/hr and the 26 cell generator current, I , is

$$w = 0.0171 I$$

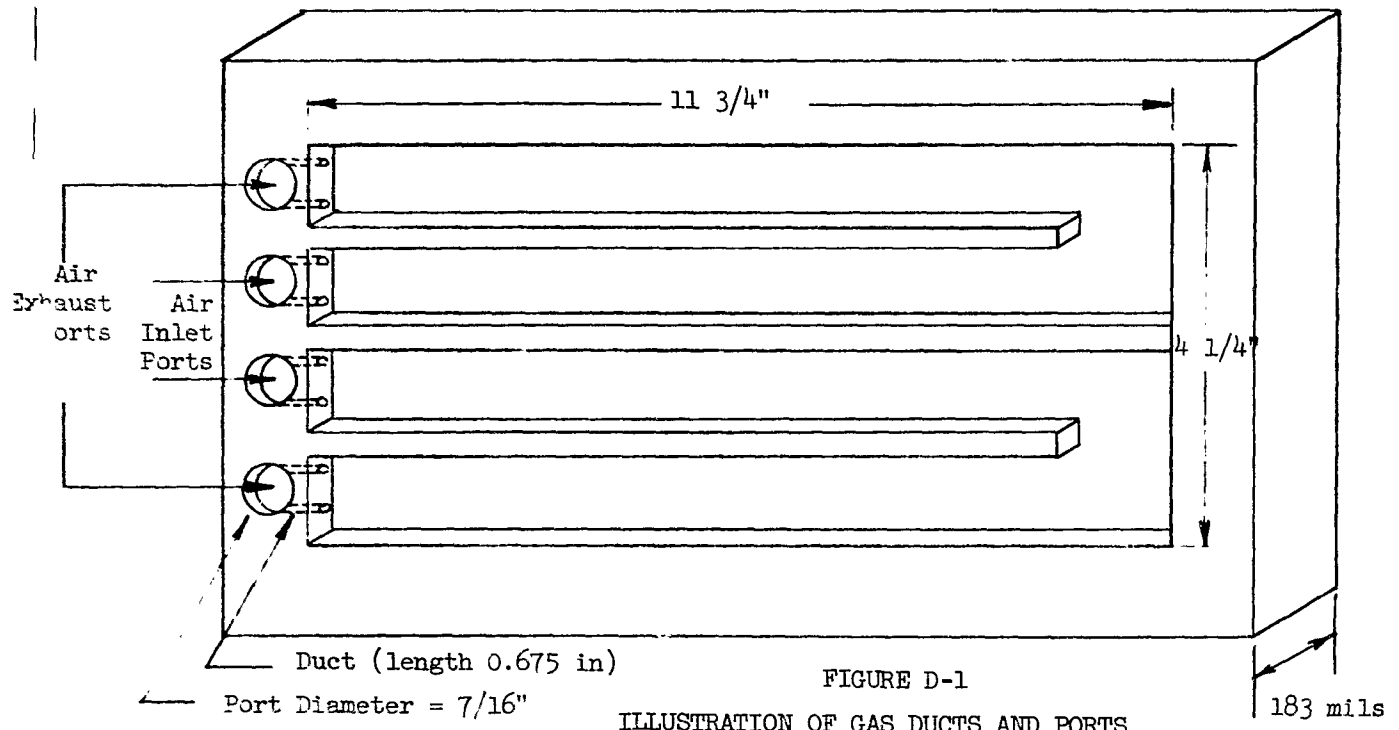


FIGURE D-1
ILLUSTRATION OF GAS DUCTS AND PORTS

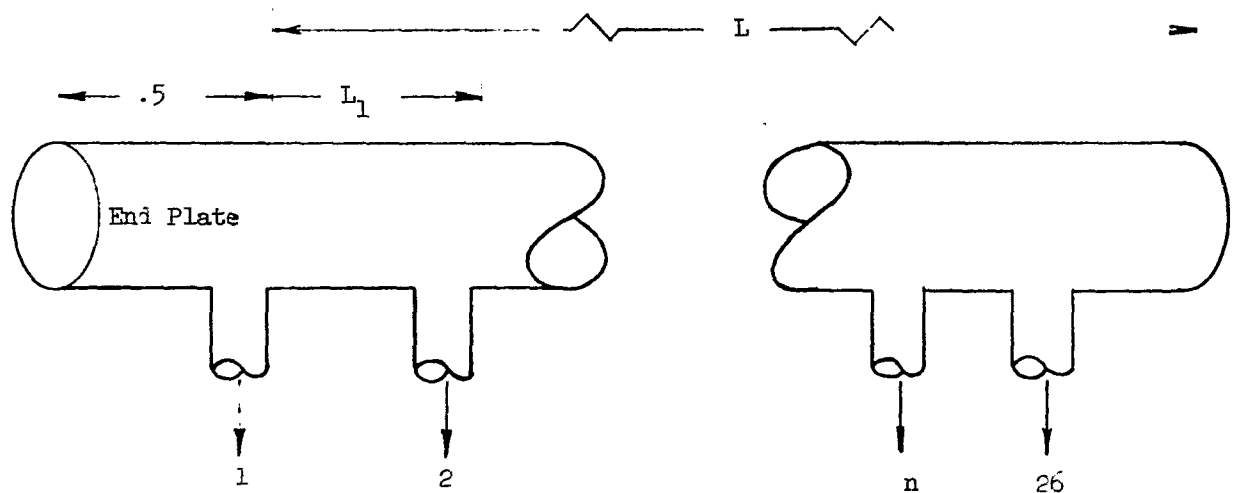


FIGURE D-2
PORT PASSAGE FORMED BY STACKING TOGETHER 26 BI-POLAR PLATES

$$Re = \frac{3.65 \times 10^{-2}}{7.10} \quad | \quad \frac{7.14 \times 10^{-2}}{1.25 \times 10^{-5}} = 1.48 \times 10^3$$

Flow is laminar, . . . laminar fluid flow relations apply.

$$\Delta P = \frac{32 \mu}{g_c D^2} (LV) \quad L = \text{passage length}$$

$$g_c = 32.2 \text{ ft/sec}^2$$

The configuration of the port passage is shown in Figure D-2.

Pressure drop from entrance of plate to first duct is:

$$\Delta P = \frac{32}{32.2} \quad | \quad \frac{1.25 \times 10^{-5}}{(3.65)^2 \times 10^{-4}} \quad | \quad 0.5 \quad | \quad 7.10$$

$$\Delta P = 2.76 \times 10^{-3} \text{ lb/ft}^2$$

For the port passage

$$\Delta P = \frac{32}{g_c D^2} (L_1 v_1 + L_2 v_2 + \dots + L_{26} v_{26})$$

$$L_1 = L_2 = \frac{L}{26}$$

$$\Delta P = \frac{32 \mu L}{g_c D^2 26} (v_1 + v_2 + \dots + v_{26})$$

$$v_2 = \frac{25}{26} v_1 \quad v_{26} = \frac{1}{26} v_1$$

$$v_3 = \frac{24}{26} v_1$$

$$\Delta P = \frac{32 \mu L}{g_c D^2 26} \quad \frac{v_1}{26} (26 + 25 + \dots + 1)$$

$$v_1 = 7.10 \text{ ft/sec}$$

$$\Delta P = \frac{32 \mu L v_1}{g_c D^2 26^2} \quad \sum_{n=1}^{n=26} n = \frac{32 \mu L v_1}{g_c D^2 26^2} \left(\frac{n(n+1)}{2} \right)$$

$$\Delta P = \frac{32}{32.2} \left| \frac{1.25 \times 10^{-5}}{(3.65)^2 \times 10^{-4}} \right| \frac{.397}{26^2} \left| \frac{7.10}{2} \right| \frac{26}{27}$$

$$\Delta P = 1.38 \times 10^{-2} \text{ lb/ft}^2$$

$$\text{Total pressure drop} = 1.38 \times 10^{-2} + 2.76 \times 10^{-3} = 1.66 \times 10^{-2} \text{ lb/ft}^2$$

The pressure drop down the duct diameter passage way should be approximately 100 times this value.

Assume duct diameter is 42 mils

$$D = \frac{42}{1000} \text{ in} = 3.5 \times 10^{-3} \text{ ft}; A = \frac{\pi D^2}{4} = \frac{\pi (3.5)^2 \times 10^{-6}}{4} = 9.26 \times 10^{-6} \text{ ft}^2$$

$$V = \frac{.892}{60} \left| \frac{2}{26} \right| \frac{2}{9.62 \times 10^{-6}} = 14.8$$

$$Re = \frac{3.5 \times 10^{-3}}{1.48 \times 10} \left| \frac{7.14 \times 10^{-2}}{1.25 \times 10^{-5}} \right| = 296$$

Flow is laminar, hence laminar flow equations apply.

Total pressure drop experienced through duct is the summation of:

Contraction pressure drop from port to duct (ΔP_1)

Pressure drop through duct (ΔP_2)

Expansion pressure drop into field of bi-polar plate (ΔP_3)
From Reference 6

$$\Delta P_1 = \frac{K_c}{2} \frac{V^2}{g_c} \rho$$

$$\Delta P_3 = \frac{K_e}{2} \frac{V^2}{g_c} \rho$$

where

$$K_c = 1.0$$

$$K_e = 1.08$$

$$\Delta P_1 + \Delta P_3 = \frac{32}{2} \left| \frac{(2.08)}{32.2} \right| \left| \frac{(14.8)^2}{(14.8)^2} \right| \left| \frac{7.14 \times 10^{-2}}{7.14 \times 10^{-2}} \right| = .504 \text{ lb/ft}^2$$

$$\Delta P_2 = \frac{32 \mu L V}{g_c D^2}$$

$$L = 0.675 \text{ in} = 5.63 \times 10^{-2} \text{ ft}$$

$$\Delta P_2 = \frac{32}{32.2} \left| \frac{1.25 \times 10^{-5}}{(3.5)^2 \times 10^{-6}} \right| \left| \frac{5.63 \times 10^{-2}}{5.63 \times 10^{-2}} \right| \left| \frac{14.8}{14.8} \right|$$

$$\Delta P_2 = 0.847$$

$$\text{Total pressure drop} = (8.47 \times 10^{-1} + 5.04 \times 10^{-1}) = 1.35$$

$$\text{Ratio of: } \frac{\text{Pressure drop through duct passage}}{\text{Pressure drop through port passage}} = \frac{1.35}{1.38 \times 10^{-2}} = 98 \approx 100$$

$$\text{Ratio} = 98 \quad 100$$

Therefore duct diameter of 42 mils is reasonable.

2) Calculation of pressure drop through generator.

The total pressure across the generator is composed of:

Contraction pressure drop from port to duct	(ΔP_1)
Pressure drop through duct	(ΔP_2)
Expansion pressure drop into field	(ΔP_3)
Pressure drop through field	(ΔP_4)
Contraction pressure drop from field to duct	(ΔP_5)
Pressure drop through duct	(ΔP_6)
Expansion pressure drop from duct to port	(ΔP_7)

For simplicity pressure drop due to pin resistance and flow path bends have been neglected.

ΔP_1 , ΔP_2 and ΔP_3 have been calculated in part "a". Since the bi-polar design is symmetrical ΔP_5 , ΔP_6 and $\Delta P_7 = \Delta P_1$, ΔP_2 and ΔP_3

$$\Delta P_4 = \frac{32 \mu L_F V_F^2}{g_c D_e^2}$$

L_F = field length

V_F = Velocity through field

D_e = equivalent diameter of flow passage

$$L_F = \frac{2 + 11.75}{12} = 1.96 \text{ ft}$$

The flow passage in the field is of rectangular shape, 1 inch wide by $1/16$ inch in depth:

$$A = \frac{\frac{1}{16} \times \frac{1}{16}}{144} = 4.34 \times 10^{-4} \text{ ft}^2$$

$$V = \frac{.892}{2} | \frac{26}{4.34 \times 10^{-4}} | \frac{60}{.663} = \frac{.663 \text{ ft}}{\text{Sec.}}$$

$$D_e = 4 \left(\frac{\frac{1}{16} \times \frac{1}{16}}{(1 + 1/16) \times (1 + 1/16)} \right) = 9.8 \times 10^{-3} \text{ ft}$$

$$\Delta P_4 = \frac{32}{32.2} | \frac{1.25 \times 10^{-5}}{(9.8)^2 \times 10^{-6}} | \frac{1.96}{.663} = \frac{.663}{\text{lb}/\text{ft}^2}$$

Total pressure drop:

$$2 (\Delta P_1 + \Delta P_2 + \Delta P_3) + \Delta P_4 = 2 (13.51 \times 10^{-1}) + 1.61 \times 10^{-1} \\ = 2.83$$

$$\Delta P_{\text{Total}} = 2.83 \text{ lb}/\text{ft}^2 = .0398 \text{ in Hg} = 0.545 \text{ in water}$$

E. HUMIDIFIER GAS PORT DESIGN

Conditions:

Air Flow: $0.892 \text{ ft}^3/\text{min}$

Temperature : 70°F (air inlet from ambient)

Pressure: 1 atm

Air is to flow through a modular assembly of 10 frames, each with the dimensions given in Figure E-1.

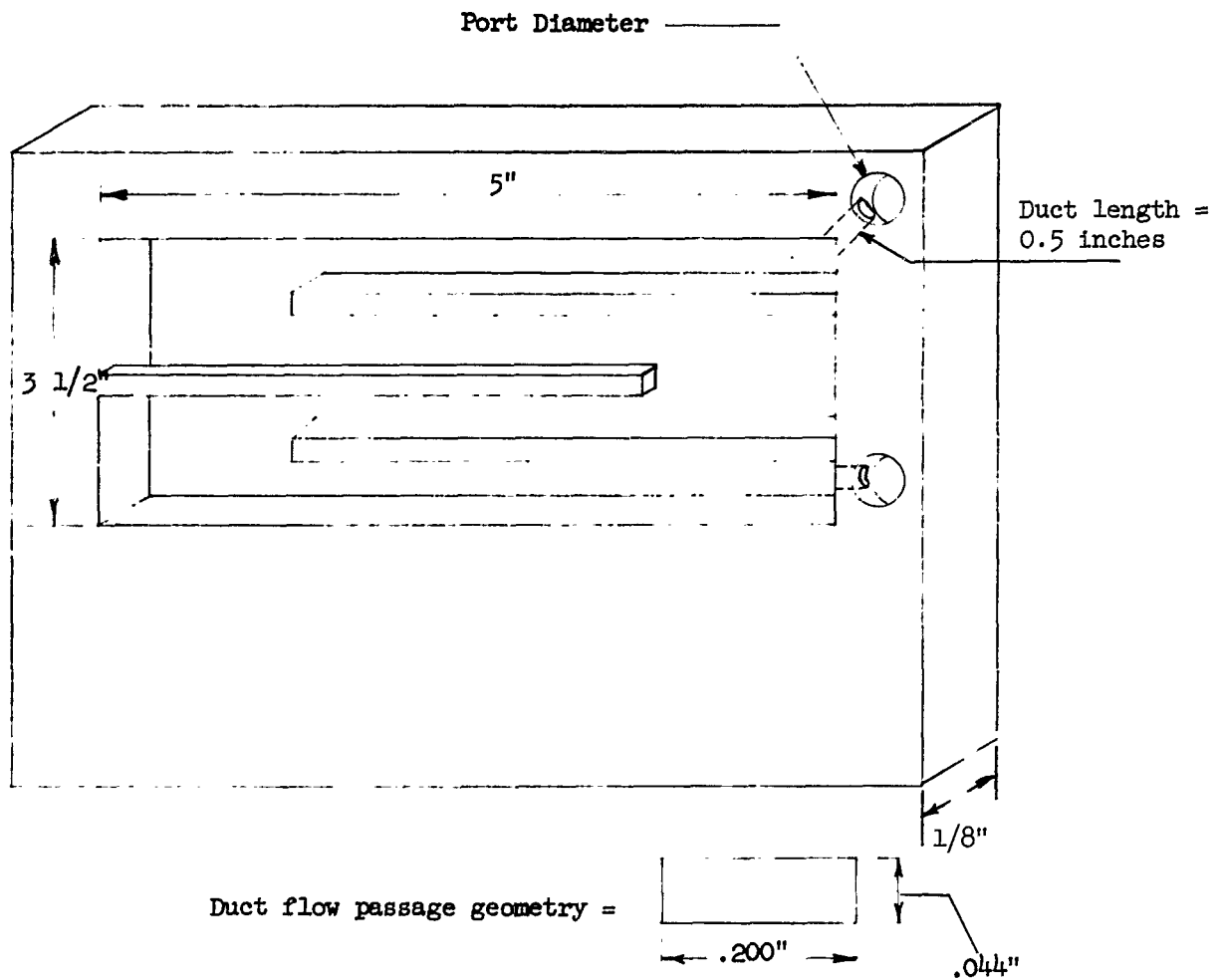


FIGURE E-1 FRAME DIAGRAM

Solution: Assume port diameter is 3/8 in.

$$A = \frac{\pi D^2}{4} = \frac{\pi (3.12)^2 \times 10^{-4}}{4} = 7.64 \times 10^{-4} \text{ ft}^2$$

$$D = 0.375 \text{ in.} = 3.12 \times 10^{-2} \text{ ft}$$

$$V = \frac{.892}{7.64 \times 10^{-4}} \Bigg|_{60} = 19.5 \text{ ft/sec}$$

$$\rho = 7.60 \times 10^{-2} \text{ lb/ft}^3$$

$$\mu = 1.20 \times 10^{-5} \text{ lb/ft sec}$$

$$Re = \frac{D V \rho}{\mu} = \frac{3.12 \times 10^{-2}}{1.20 \times 10^{-5}} \Bigg|_{19.5} \Bigg|_{7.60 \times 10^{-2}}$$

Flow is laminar, therefore, pressure drop equations outlined in the generator gasport design calculations are also applicable to this portion of the design.

Thickness of humidifier endplate = 0.5 in.

$$\Delta P = \frac{32 \mu L V}{g_c D^2} = \text{pressure drop through endplate}$$

$$\Delta P = \frac{32}{32.2} \Bigg| \frac{1.20 \times 10^{-5}}{(3.12)^2 \times 10^{-4}} \Bigg| \frac{.5}{12} \Bigg| \frac{19.5}{12} = 9.94 \times 10^{-3} \text{ lbs/ft}^2$$

The pressure drop through the duct passage or manifold is:

$$\Delta P = \frac{32 \mu L V_1}{g_c D^2 (10^2)} \frac{[n(n+1)]}{2}$$

$$L = \frac{10}{12} \Bigg| \frac{1/8 \text{ in}}{12} \Bigg| = .104$$

$$\Delta P = \frac{32}{32.2} \left| \frac{1.20 \times 10^{-5}}{(3.2)^2 \times 10^{-4}} \right| \frac{.104}{100} \left| \frac{10}{2} \right| \frac{11}{1}$$

$$\text{Total pressure drop} = (7.04 \times 10^{-4} + 99.4 \times 10^{-4}) = \\ 1.06 \times 10^{-2} \text{ lb/in}^2$$

If port hole is properly specified, the pressure drop down the ducting passage will be approximately 100 times this value.

$$D_e \text{ for duct passage} = \frac{4 \left(.044 \times .200 \right)}{\left(.044 + .200 + .044 + .200 \right)} \frac{1}{12}$$

$$V = \frac{0.892 \text{ ft}^3}{60 \text{ sec.}} \left| \frac{144}{0.044 \times 0.20} \right| \frac{1}{60} = 24.4 \text{ ft/sec.}$$

$$Re = \frac{D_e V \rho}{\mu} = \frac{6.03 \times 10^{-3}}{1.20 \times 10^{-5}} \frac{2.44 \times 10}{7.60 \times 10^{-2}} = 92.8$$

Flow is laminar and equations listed in the generator gas port design calculations are also applicable for this portion of the design.

$$\Delta P_1 + \Delta P_3 = (K_c + K_e) \frac{V^2 \rho}{2 g_c}$$

$$\Delta P_1 + \Delta P_3 = \frac{(2.08)}{2} \left| \frac{(2.44)^2 \times 10^2}{32.2} \right| \frac{7.60 \times 10^{-2}}{1}$$

$$\Delta P_1 + \Delta P_3 = 1.47 \text{ lb/ft}^2$$

$$\Delta P_2 = \frac{32 \mu L V}{g_c D_e^2}$$

$$L = \frac{.5 \text{ in}}{12} = 4.17 \times 10^{-2} \text{ ft}$$

$$\Delta P_2 = \frac{32}{32.2} \left| \frac{1.20 \times 10^{-5}}{(6.03)^2 \times 10^{-6}} \right| \frac{4.17 \times 10^{-2}}{1} \frac{2.44 \times 10}{1} \\ = 3.35 \times 10^{-1} \text{ lb/ft}^2$$

$$\text{Total ducting pressure drop} = 1.47 + 0.34 = 1.81 \text{ lb/ft}^2$$

$$\text{Ratio of } \frac{\text{pressure drop through duct passage}}{\text{pressure drop through port passage}} = \frac{1.81}{9.94 \times 10^{-3}} = 182$$

This ratio is 100 or greater, therefore, an inlet port diameter of 3/8 inch was a proper choice.

F. COOLANT AIR DUCTING DESIGN

The following calculational procedure was used in designing the coolant air ducting system.

Total flow rate of air required: 116 SCFM

This value is calculated as follows:

The design conditions for the generator were:

current = 11.7 amps

maximum cell voltage = 1.2 volts

number of cells = 26

$$\text{Maximum generator heat load} = \frac{11.7}{\text{amps}} \times \frac{1.2}{\text{volts}} \times \frac{26}{\text{cells}} = 366 \text{ watts or} \\ 20.8 \text{ BTU/min.}$$

$$\text{Air cooling rate (w)} = \frac{q}{c_p \Delta T}$$

$$c_p = .226 \frac{\text{BTU}}{\text{F}}$$

$$\Delta T = 10^\circ\text{F (assumed)}$$

$$w = \frac{20.8}{.226} \times \frac{1}{10} = 9.22 \frac{\text{lb}}{\text{min}} \approx 116 \text{ SCFM}$$

Air is to be divided into two streams. One half of the air flow cools front bipolar plate fins. Remaining air flow cools back bipolar plate fins.

The cooling air enters tangent to the fin passages. A Plexiglas strip with circular holes that are in the center of each of the fin passageways is placed parallel to the air flow direction. The design problem is to specify the hole diameters in the Plexiglas so that equal air flow passes through each of the fin passageways of the bipolar plates. The dimensions of the flow chamber are given in Figure F-1

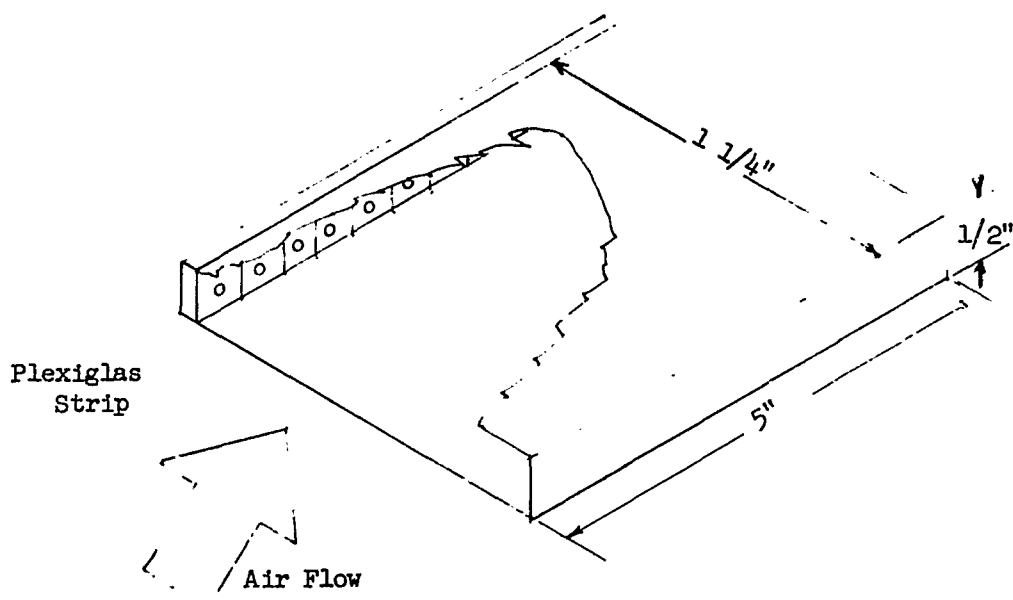


FIGURE F-1
DIMENSIONAL DIAGRAM OF COOLING AIR PASSAGE

$$\text{Flow Area: } \frac{1 \frac{1}{4} \times 1/2}{144} = 4.34 \times 10^{-2} \text{ ft}^2$$

$$D_e = \frac{4(1 \frac{1}{4} \times 1/2)}{(1 \frac{1}{4} + 1/2 + 1 \frac{1}{4} + 1/2)} \frac{1}{12}$$

$$D_e = 5.96 \times 10^{-2} \text{ ft}$$

$$V = \frac{116 \text{ ft}^3}{2} \left| \frac{60}{4.34 \times 10^{-2}} \right. = 223 \text{ ft/sec.}$$

$$\rho = 7.60 \times 10^{-2} \text{ lb/ft}^3$$

$$\mu = 1.20 \times 10^{-5} \text{ lb/ft-sec}$$

$$Re = \frac{D_e V \rho}{\mu} = \frac{5.96 \times 10^{-2}}{1.20 \times 10^{-5}} \left| \frac{223}{7.60 \times 10^{-2}} \right. = 8.43 \times 10^4$$

$$Re = 8.43 \times 10^4$$

This is a turbulent value of the Reynold's number and, therefore, a set of equations different from those used in preceding sections are needed to determine the pressure drop along the air passageway (See Figure F-2).

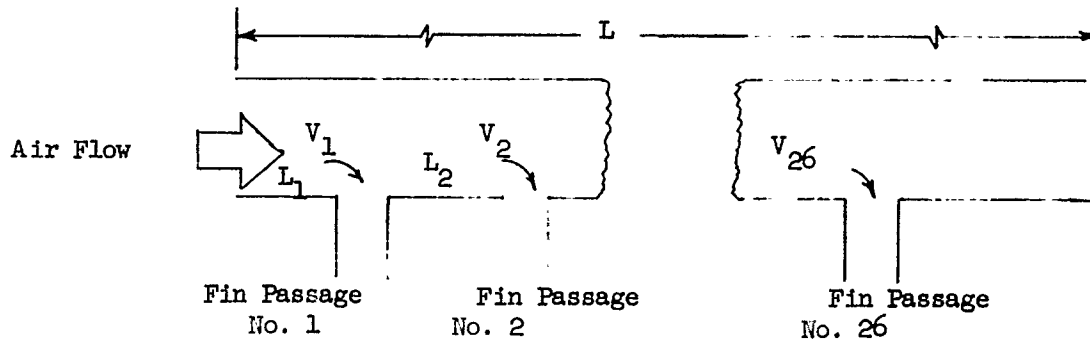


FIGURE F-2
COOLING GAS PASSAGE

$$P = \frac{2\lambda \rho}{D_e g_c} \sum_{n=1}^{n=26} (L_n v_n^2) = \frac{2\lambda \rho}{D_e g_c} (L_1 v_1^2 + L_2 v_2^2 + \dots + L_{26} v_{26}^2)$$

λ = friction factor

$$L_1 = L_2 = \frac{L}{26}$$

$$\Delta P = \frac{2\lambda \rho L}{D_e g_c 26} (v_1^2 + v_2^2 + \dots + v_{26}^2)$$

$$v_2 = \frac{25}{26} v_1 ; \quad v_2^2 = \frac{(25)^2}{(26)^2} v_1^2$$

$$v_{26} = \frac{1}{26} v_1 ; \quad v_{26}^2 = \frac{1^2}{26^2} v_1^2$$

$$\Delta P = \frac{2\lambda \rho L v_1^2}{D_e g_c 26^3} (26^2 + 25^2 + \dots + 1^2)$$

$$\Delta P = \frac{2\lambda \rho L v_1^2}{D_e g_c 26^3} \sum_{n=1}^{n=26} n^2$$

$$\Delta P = \frac{2\lambda \rho L v_1^2}{D_e g_c 26^3} \frac{n(n+1)(2n+1)}{6}$$

For a Reynold's number of 8.43×10^4 and assuming the flow passage is smooth (6)

$$\lambda = 4.7 \times 10^{-3}$$

$$L = \frac{5 \text{ in}}{12} = 4.17 \times 10^{-1} \text{ ft}$$

$$\Delta P = \frac{2}{5.96 \times 10^{-2}} \left| \frac{4.7 \times 10^{-3}}{3.22 \times 10} \right| \left| \frac{7.60 \times 10^{-2}}{(2.6)^3 \times 10^3} \right| \left| \frac{4.17 \times 10^{-1}}{6} \right| \left| \frac{(2.23)^2 \times 10^4}{x} \right|$$

$$\Delta P = \frac{2.6 \times 10}{2.7 \times 10} \left| \frac{5.3 \times 10}{\Delta P} \right|^2$$

$$\Delta P = 2.71 \text{ lb/ft}^2$$

The pressure drop through the hole in the Plexiglas strip should be approximately 100 times this value, in order to assure equal air flow distribution along each of the fin passages. In turbulent flow the hole in the strip can be treated as an orifice. If the linear velocity entering the orifice is small in comparison with the velocity through the orifice, the pressure drop is:

$$\Delta P = \frac{V^2 \rho}{C_o^2 2 g_c}$$

This is a reasonable assumption for this design.

$$C_o = \text{orifice coefficient} \approx 6.1 \times 10^{-1} \text{ (assumed)}$$

Assume the orifice opening is : 0.1 inches in diameter

$$V = \frac{58 \text{ ft}^3}{26 \text{ min}} \approx 6.85 \times 10^2 \text{ ft/sec}$$

$$\Delta P = \frac{(6.85)^2 \times 10^4}{(6.1)^2 \times 10^{-2}} \left| \frac{7.60 \times 10^{-2}}{2} \right| \left| \frac{}{3.22 \times 10} \right| = 1.49 \times 10^3$$

$$\text{Ratio of } \frac{\text{pressure drop through orifice}}{\text{pressure drop through flow passage}} = \frac{1.49 \times 10^3}{2.71} = 550$$

The ratio of 100 or greater was met and therefore the orifice size of 0.1 inches was appropriate.

UNCLASSIFIED

Security Classification

DOCUMENT CONTROL DATA - R&D

(Security classification of title, body of abstract and indexing annotation must be entered when the overall report is classified)

1. ORIGINATING ACTIVITY (Corporate author) TRW Electromechanical Division Thompson-Ramo-Wooldridge, Inc. 23555 Euclid Ave., Cleveland, Ohio 44117		2a. REPORT SECURITY CLASSIFICATION UNCLASSIFIED
		2b. GROUP
3. REPORT TITLE Experimental Oxygen Concentrating System		
4. DESCRIPTIVE NOTES (Type of report and inclusive dates) Final Technical Report, July 1964 through February 1965		
5. AUTHOR(S) (Last name, first name, initial) Wynveen, Dr. Richard A. Montgomery, Keith M.		
6. REPORT DATE April 1965	7a. TOTAL NO. OF PAGES 79	7b. NO. OF REFS / Six (6)
8a. CONTRACT OR GRANT NO. AF 33(615)-1856	9a. ORIGINATOR'S REPORT NUMBER(S) TRW ER-6411	
b. PROJECT NO. 6146	9b. OTHER REPORT NO(S) (Any other numbers that may be assigned this report) AFTDL-TR-65-32	
c. Task No. 614603		
d.		
10. AVAILABILITY/LIMITATION NOTICES - Qualified users may obtain copies of this report from the DDC. Foreign announcement and dissemination of this report is not authorized. DDC release to EFSTI is not authorized.		
11. SUPPLEMENTARY NOTES	12. SPONSORING MILITARY ACTIVITY Air Force Flight Dynamics Laboratory Wright-Patterson Air Force Base, Ohio	
13. ABSTRACT - A program to design, fabricate, and test a laboratory model of an oxygen concentrator, capable of generating 0.20 lb/hr of pure oxygen by electro-chemically concentrating it from air, was successfully conducted. The fabricated model consisted of 26 series-connected cells. Four of the cells, tested before incorporation into the 26-cell unit, demonstrated an oxygen generation rate of 0.10 lb/hr. A 26-cell unit operating at an equivalent unit cell output would produce nearly 0.68 lb/hr, over three times the design level. The 26-cell unit itself was operated at a maximum output of about 0.56 lb/hr for only a short period of time because the heat generated was in excess of the heat removal systems' capacity. At the completion of the contractual test program, over 700 hours had been accumulated on the original four cells, about 345 hours of which were logged while functioning as part of the 26-cell unit. The concentrator was shown to function properly at 6.5 - 15.5 psia pressures, with little variation in the power required for a given oxygen output. For optimum performance, the generator required an air flowrate of at least 2.5 times the theoretical minimum. Oxygen purity was over 99.5%. The laboratory model weighs about 28 pounds and consumes 240-300 watts of power at 0.2 lb/hr oxygen output. Also included in this program was the design, fabrication, and testing of a humidifier that would operate under airborne conditions. Instrumentation was provided for measuring and controlling gas flows, pressures, temperatures, and dew points and for monitoring cell voltages.		

UNCLASSIFIED**Security Classification**

14. KEY WORDS	LINK A		LINK B		LINK C	
	ROLE	WT.	ROLE	WT.	ROLE	WT.
Electrochemistry Electrochemical Cells Oxygen generation, Oxygen concentration Oxygen supply systems Aviator's oxygen						
INSTRUCTIONS						
1. ORIGINATING ACTIVITY: Enter the name and address of the contractor, subcontractor, grantee, Department of Defense activity or other organization (corporate author) issuing the report.	imposed by security classification, using standard statements such as:					
2a. REPORT SECURITY CLASSIFICATION: Enter the overall security classification of the report. Indicate whether "Restricted Data" is included. Marking is to be in accordance with appropriate security regulations.	(1) "Qualified requesters may obtain copies of this report from DDC."					
2b. GROUP: Automatic downgrading is specified in DoD Directive 5200.10 and Armed Forces Industrial Manual. Enter the group number. Also, when applicable, show that optional markings have been used for Group 3 and Group 4 as authorized.	(2) "Foreign announcement and dissemination of this report by DDC is not authorized."					
3. REPORT TITLE: Enter the complete report title in all capital letters. Titles in all cases should be unclassified. If a meaningful title cannot be selected without classification, show title classification in all capitals in parenthesis immediately following the title.	(3) "U. S. Government agencies may obtain copies of this report directly from DDC. Other qualified DDC users shall request through _____"					
4. DESCRIPTIVE NOTES: If appropriate, enter the type of report, e.g., interim, progress, summary, annual, or final. Give the inclusive dates when a specific reporting period is covered.	(4) "U. S. military agencies may obtain copies of this report directly from DDC. Other qualified users shall request through _____"					
5. AUTHOR(S): Enter the name(s) of author(s) as shown on or in the report. Enter last name, first name, middle initial. If military, show rank and branch of service. The name of the principal author is an absolute minimum requirement.	(5) "All distribution of this report is controlled. Qualified DDC users shall request through _____"					
6. REPORT DATE: Enter the date of the report as day, month, year; or month, year. If more than one date appears on the report, use date of publication.	If the report has been furnished to the Office of Technical Services, Department of Commerce, for sale to the public, indicate this fact and enter the price, if known.					
7a. TOTAL NUMBER OF PAGES: The total page count should follow normal pagination procedures, i.e., enter the number of pages containing information.	11. SUPPLEMENTARY NOTES: Use for additional explanatory notes.					
7b. NUMBER OF REFERENCES: Enter the total number of references cited in the report.	12. SPONSORING MILITARY ACTIVITY: Enter the name of the departmental project office or laboratory sponsoring (paying for) the research and development. Include address.					
8a. CONTRACT OR GRANT NUMBER: If appropriate, enter the applicable number of the contract or grant under which the report was written.	13. ABSTRACT: Enter an abstract giving a brief and factual summary of the document indicative of the report, even though it may also appear elsewhere in the body of the technical report. If additional space is required, a continuation sheet shall be attached.					
8b, 8c, & 8d. PROJECT NUMBER: Enter the appropriate military department identification, such as project number, subproject number, system numbers, task number, etc.	It is highly desirable that the abstract of classified reports be unclassified. Each paragraph of the abstract shall end with an indication of the military security classification of the information in the paragraph, represented as (TS), (S), (C), or (U).					
9a. ORIGINATOR'S REPORT NUMBER(S): Enter the official report number by which the document will be identified and controlled by the originating activity. This number must be unique to this report.	There is no limitation on the length of the abstract. However, the suggested length is from 150 to 225 words.					
9b. OTHER REPORT NUMBER(S): If the report has been assigned any other report numbers (either by the originator or by the sponsor), also enter this number(s).	14. KEY WORDS: Key words are technically meaningful terms or short phrases that characterize a report and may be used as index entries for cataloging the report. Key words must be selected so that no security classification is required. Identifiers, such as equipment model designation, trade name, military project code name, geographic location, may be used as key words but will be followed by an indication of technical context. The assignment of links, rules, and weights is optional.					
10. AVAILABILITY/LIMITATION NOTICES: Enter any limitations on further dissemination of the report, other than those						

UNCLASSIFIED**Security Classification**